



QEX

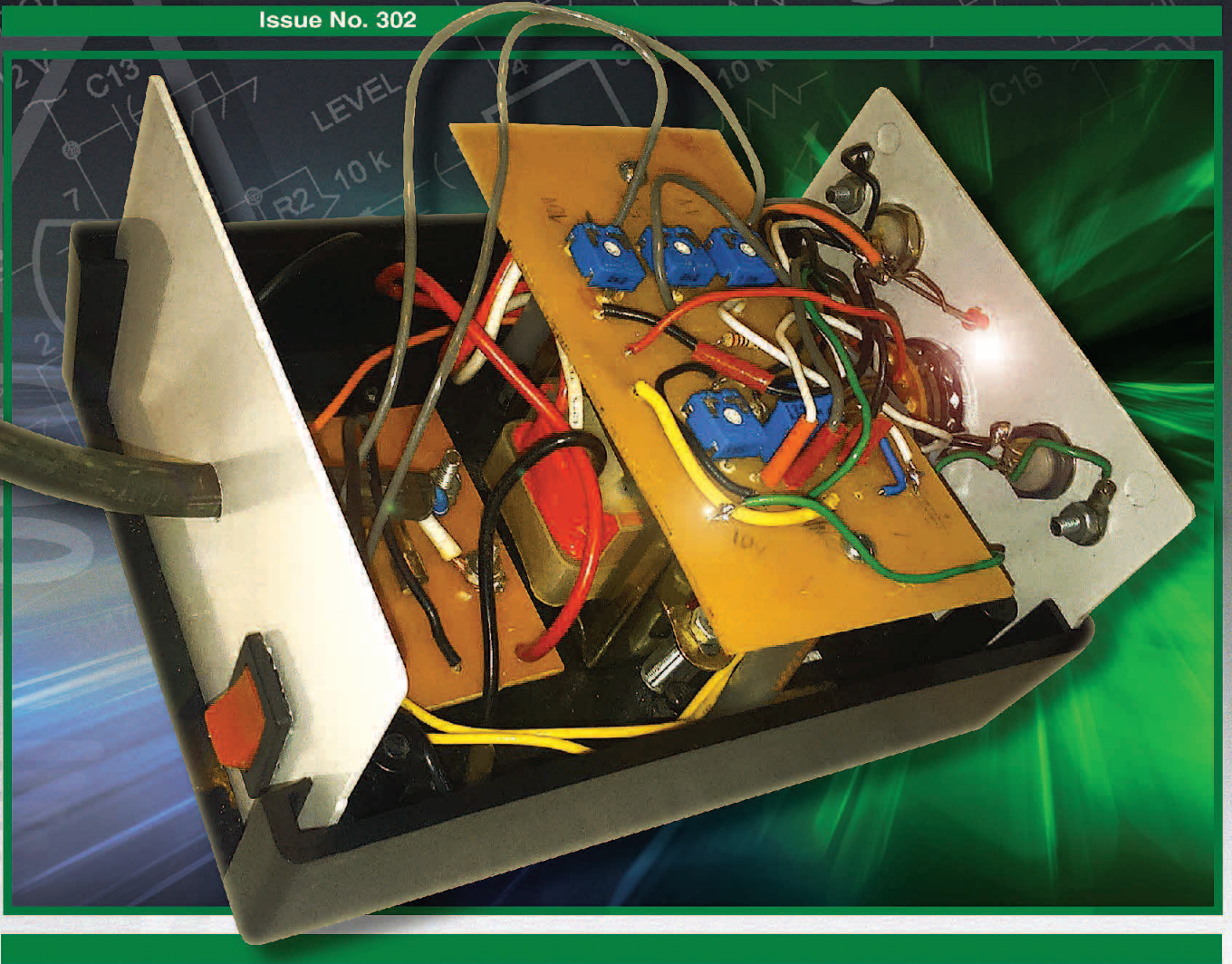
May/June 2017

www.arrl.org

\$7

A Forum for Communications Experimenters

Issue No. 302



PY3PR curve tracer provides selectable scanning voltages from a single-voltage transformer.

New

APRS® / D-STAR®

TH-D74A 144/220/430 MHz Tribander

Introducing the TH-D74A for the ultimate in APRS and D-STAR performance. KENWOOD has already garnered an enviable reputation with the TH-D72A handheld APRS amateur radio transceiver. And now it has raised the bar even further with the new TH-D74A, adding support for D-STAR, the digital voice & data protocol developed by the JARL, and enabling simultaneous APRS and D-STAR operation – an industry first.



- ▶ APRS compliance using packet communication to exchange real-time GPS position information and messages
- ▶ Compliant with digital/voice mode D-STAR digital amateur radio networks
- ▶ Built-in high performance GPS unit with Auto Clock Setting
- ▶ Wide-band and multi-mode reception
- ▶ 1.74" (240 x 180 pixel) Transflective color TFT display
- ▶ IF Filtering for improved SSB/CW/AM reception
- ▶ High performance DSP-based audio processing & voice recording
- ▶ Compliant with Bluetooth, microSD & Micro-USB standards
- ▶ External Decode function (PC Decode 12kHz IF Output, BW:15 kHz)
- ▶ Free software for Memory and Frequency Control Program
- ▶ Data Import / Export (Digital Repeater List, Call sign, Memory Channel)
- ▶ Four TX Power selections (5/2/0.5/0.05 W)
- ▶ Dust and Water resistant IP54/55 standards

APRS (The Automatic Packet Reporting System) is a registered American trademark of WB4APR (Mr. Bob Bruninga). D-Star is a digital radio protocol developed by JARL (Japan Amateur Radio League).

KENWOOD

Customer Support/Distribution Customer Support:
(310) 639-4200 Fax: (310) 537-8235

www.kenwood.com/usa



ADS#29016

QEX (ISSN: 0886-8093) is published bimonthly in January, March, May, July, September, and November by the American Radio Relay League, 225 Main Street, Newington, CT 06111-1494. Periodicals postage paid at Hartford, CT and at additional mailing offices.

POSTMASTER: Send address changes to: QEX, 225 Main St, Newington, CT 06111-1494 Issue No 302

Publisher
American Radio Relay League

Kazimierz "Kai" Siwiak, KE4PT
Editor

Lori Weinberg, KB1EIB
Assistant Editor

Zack Lau, W1VT
Ray Mack, W5IFS
Contributing Editors

Production Department

Steve Ford, WB8IMY
Publications Manager

Michelle Bloom, WB1ENT
Production Supervisor

Sue Fagan, KB1OKW
Graphic Design Supervisor

David Pingree, N1NAS
Senior Technical Illustrator

Brian Washing
Technical Illustrator

Advertising Information Contact:

Janet L. Rocco, W1JLR
Business Services
860-594-0203 – Direct
800-243-7768 – ARRL
860-594-4285 – Fax

Circulation Department

Cathy Stepina, QEX Circulation

Offices

225 Main St, Newington, CT 06111-1494 USA
Telephone: 860-594-0200
Fax: 860-594-0259 (24 hour direct line)
e-mail: qex@arrl.org

Subscription rate for 6 issues:

In the US: \$29;

US by First Class Mail: \$40;

International and Canada by Airmail: \$35

Members are asked to include their membership control number or a label from their QST when applying.

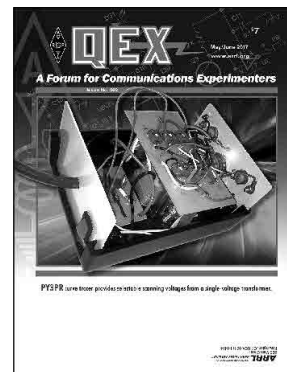
In order to ensure prompt delivery, we ask that you periodically check the address information on your mailing label. If you find any inaccuracies, please contact the Circulation Department immediately. Thank you for your assistance.



Copyright © 2017 by the American Radio Relay League Inc. For permission to quote or reprint material from QEX or any ARRL publication, send a written request including the issue date (or book title), article, page numbers and a description of where you intend to use the reprinted material. Send the request to the office of the Publications Manager (permission@arrl.org).

About the Cover

Paulo Renato F. Ferreira, PY3PR, designed an improved V/I curve tracer to perform in-circuit trouble shooting using a tester that provides selectable scanning voltages for testing. The circuit uses a transformer that has a single-voltage secondary winding that supports three ranges of scanning voltages.



In This Issue

Features

2 Perspectives
Kazimierz "Kai" Siwiak, KE4PT

3 The DG5MK IV Meter — An Accurate Antenna Analyzer
Michael Knitter, DG5MK

16 Improve Performance of Your Octopus V/I Curve Tracer Using a Single Voltage Transformer
Paulo Renato F. Ferreira, PY3PR

21 Octave for Complex Characteristic Impedance
Maynard A. Wright, W6PAP

26 Polarization in HF Atmospheric Noise
Robert H. Sternowski, WB0LBI

27 Book Review
Kai Kiwiak, KE4PT

28 Technical Note

30 Letters to the Editor

Index of Advertisers

ARRL.....32, Cover III
DX Engineering: 15
Kenwood Communications:Cover II
Nemal Electronics International, Inc: 29

RF Parts:.....29, 31
SteppIR.....Cover IV
Tucson Amateur Packet Radio:20

The American Radio Relay League



The American Radio Relay League, Inc. is a noncommercial association of radio amateurs, organized for the promotion of interest in Amateur Radio communication and experimentation, for the establishment of networks to provide communications in the event of disasters or other emergencies, for the advancement of the radio art and of the public welfare, for the representation of the radio amateur in legislative matters, and for the maintenance of fraternalism and a high standard of conduct.

ARRL is an incorporated association without capital stock chartered under the laws of the state of Connecticut, and is an exempt organization under Section 501(c)(3) of the Internal Revenue Code of 1986. Its affairs are governed by a Board of Directors, whose voting members are elected every three years by the general membership. The officers are elected or appointed by the Directors. The League is noncommercial, and no one who could gain financially from the shaping of its affairs is eligible for membership on its Board.

"Of, by, and for the radio amateur," ARRL numbers within its ranks the vast majority of active amateurs in the nation and has a proud history of achievement as the standard-bearer in amateur affairs.

A *bona fide* interest in Amateur Radio is the only essential qualification of membership; an Amateur Radio license is not a prerequisite, although full voting membership is granted only to licensed amateurs in the US.

Membership inquiries and general correspondence should be addressed to the administrative headquarters:

ARRL
225 Main Street
Newington, CT 06111 USA
Telephone: 860-594-0200
FAX: 860-594-0259 (24-hour direct line)

Officers

President: Rick Roderick, K5UR
PO Box 1463, Little Rock, AR 72203

Chief Executive Officer: Tom Gallagher, NY2RF

The purpose of QEX is to:

- 1) provide a medium for the exchange of ideas and information among Amateur Radio experimenters,
- 2) document advanced technical work in the Amateur Radio field, and
- 3) support efforts to advance the state of the Amateur Radio art.

All correspondence concerning *QEX* should be addressed to the American Radio Relay League, 225 Main Street, Newington, CT 06111 USA. Envelopes containing manuscripts and letters for publication in *QEX* should be marked Editor, *QEX*.

Both theoretical and practical technical articles are welcomed. Manuscripts should be submitted in word-processor format, if possible. We can redraw any figures as long as their content is clear. Photos should be glossy, color or black-and-white prints of at least the size they are to appear in *QEX* or high-resolution digital images (300 dots per inch or higher at the printed size). Further information for authors can be found on the Web at www.arrl.org/qex/ or by e-mail to qex@arrl.org.

Any opinions expressed in *QEX* are those of the authors, not necessarily those of the Editor or the League. While we strive to ensure all material is technically correct, authors are expected to defend their own assertions. Products mentioned are included for your information only; no endorsement is implied. Readers are cautioned to verify the availability of products before sending money to vendors.

Kazimierz "Kai" Siwiak, KE4PT

Perspectives

Institutional Memory

Amateur Radio operators have accumulated a huge collective *institutional memory* of data, information, and knowledge about Amateur Radio techniques and technology. Although we strive to cover a wide range of current technologies and topics from that evolving *memory* in these pages, the typical article can span several pages and cover topics in extended depth. Full-length articles require much effort by our authors, and producing a long in-depth technical study might not be for everyone. Yet there are ideas out there, technical treasures, which might be described briefly. So how can we tap into this aspect of the *institutional memory*? How can we elicit *QEX*-level technical tidbits from our readers? Going forward a new **Technical Note** column debuts in *QEX*.

By all means, keep the full-length *QEX* articles flowing in, but let's also tap into our *institutional memory* and share a brief **Technical Note** that is perhaps several hundred words long plus a figure or two. Expand on another author's work and add to the Amateur Radio *institutional memory* with your technical observation. Let us know that your submission is intended as a **Note**.

In This Issue

Our authors improve on several instances of test equipment, rediscover old noise measurements, and beef up transmission line analysis.

Michael Knitter, DG5MK, describes a complex-impedance analyzer that uses a heterodyning technique and high resolution ADCs to get good accuracy at low cost.

Robert H. Sternowski, WB0LBI, uncovers old measurements, which show that vertically and horizontally polarized noise can differ by tens of decibels in the lower HF bands.

Paulo Renato F. Ferreira, PY3PR, updates the Octopus V/I curve trace by providing selectable scanning voltages for testing.

Maynard A. Wright, W6PAP, provides Octave software for computing the performance of transmission lines having a complex characteristic impedance.

QEX is edited by Kazimierz "Kai" Siwiak, KE4PT, (ksiwiak@arrl.org) and is published bimonthly. *QEX* is a forum for the free exchange of ideas among communications experimenters. The content is driven by you, the reader and prospective author. The subscription rate (6 issues per year in the United States is \$29. First Class delivery in the US is available at an annual rate of \$40. For international subscribers, including those in Canada and Mexico, *QEX* can be delivered by airmail for \$35 annually. Subscribe today at www.arrl.org/qex.

Would you like to write for *QEX*? We pay \$50 per published page. Get more information and an Author Guide at www.arrl.org/qex-author-guide. If you prefer postal mail, send a business-size self-addressed, stamped (US postage) envelope to: *QEX* Author Guide, c/o Maty Weinberg, ARRL, 225 Main St, Newington, CT 06111.

73,

Kazimierz "Kai" Siwiak, KE4PT

The DG5MK IV Meter — An Accurate Antenna Analyzer

This complex-impedance analyzer uses a heterodyning technique and high resolution ADCs to get good accuracy at low cost.

One of the most needed measurement instruments for Amateur Radio is an affordable antenna analyzer. This article describes a high-accuracy handheld, low cost 100 MHz analyzer (Figure 1). It allows new and experienced do-it-yourself (DIY) Amateur Radio operators to not only check antennas for correct tuning, but also for measuring impedances in many other areas of Amateur Radio. An analyzer can measure the impedance of the antenna without applying several watts of RF power into an antenna to check SWR, as required with traditional SWR meters. However, these instruments are either expensive, or lack accuracy and functionality.

The DG5MK IV Meter is a very affordable true RF I-V (current-voltage) analyzer with short, open, load compensation (SOL) to allow professional measurements in a broad variety of configurations from 100 kHz to 100 MHz. The described basic version has a 2-line LCD display with basic functionality. There are plans to add a graphical LCD display version with additional features.

We start with some theory on impedance measurement. All of the building blocks from generating the measurement signal up to impedance calculation will be discussed and evaluated. Skip this part if you are not interested in the theory and mathematics. The second part deals with the actual implementation of the I-V meter. Hints for building will be followed by practical measurements, technical data and a look at accuracy.

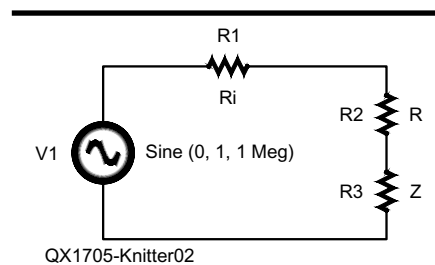
Impedance Measurement in General

Checking antenna SWR is a matter of finding how well the impedance of



Figure 1 — An image of the DG5MK IV-Meter antenna analyzer.

the antenna system is aligned with the characteristic feed line impedance, Z_0 . For most Amateur Radio applications Z_0 is 50 Ω (for cable TV the standard is 75 Ω). Maximum power will be transferred from the transceiver to the antenna when there are no reflected waves coming back from the antenna. More on analyzer basics and measuring impedance can be found on Internet searches.^{1,2} Most methods focus on measuring the voltage along, and the current through the device under test (DUT). Z could represent an antenna in Figure 2.



QX1705-Knitter02

Figure 2 — Determine impedance Z by measuring currents in R and voltage across Z .

We apply Ohm's law according to Equation (1). Instead of measuring the current, I , through Z we can measure the voltage, U , along a well-known resistor R in series to Z .

$$Z = \frac{U_Z}{I_Z} = R \frac{U_Z}{U_R} \quad (1)$$

Antenna systems and other impedances have capacitive and inductive components as well. Figure 3 shows four different equivalent circuits to illustrate this. The two top circuits have a capacitor or inductor attached in series. The new total Z has a series equivalent circuit. The two bottom circuits use a parallel model. At a given frequency one can be calculated from the other.

If antennas have a capacitive component in their impedance they are usually physically too short relative to a wavelength. For an inductive component, they are usually too long. If they have exactly the right size, the C or L will disappear leaving only the resistive part. This resistive part is not necessarily 50Ω , depending on the type and height of the antenna above ground. Additional LC networks and/or transformers (antenna tuners) are used to transform the antenna resistance to 50Ω . Including a capacitive or inductive component makes the impedance complex.

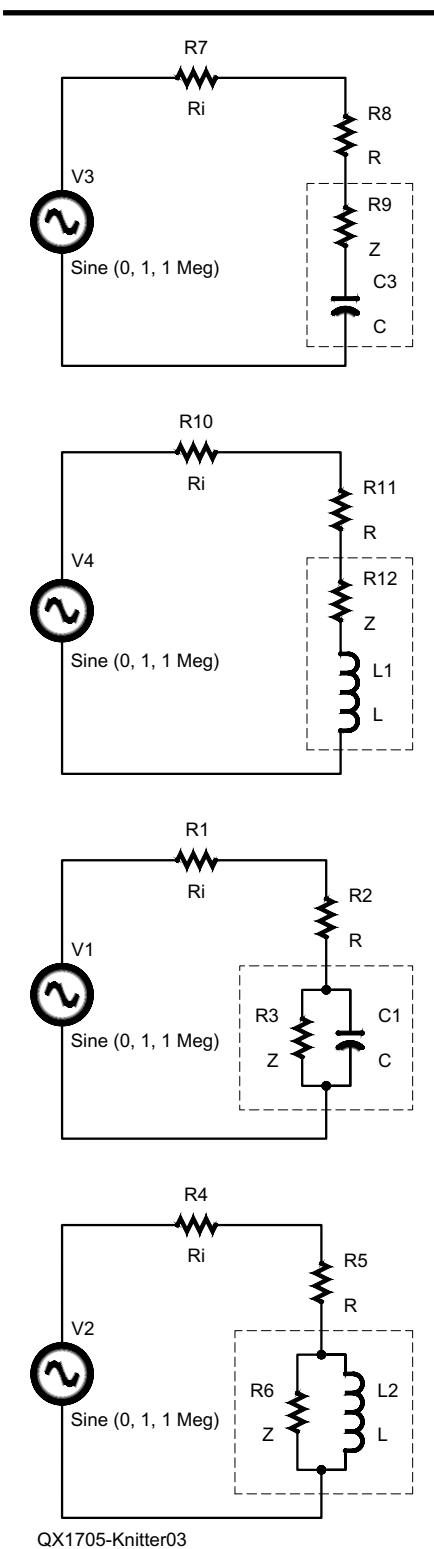


Figure 3 — Equivalent circuits for complex impedances.

Impedance goes Complex

A basic property for a capacitor is that the voltage will lag the current. For inductors the

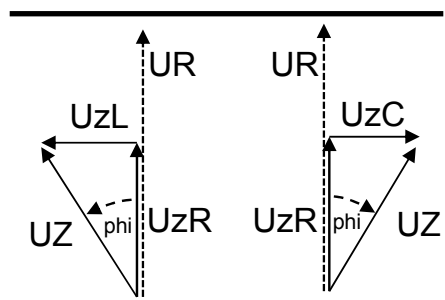


Figure 4 — Voltage relationships for series equivalent circuits of complex impedances.

current will lag the voltage. What this means is that voltage and current are out of phase for a capacitor or an inductor. For an ideal capacitor or inductor the phase difference is 90 degrees (or $\pi/2$ radians). For the series equivalent circuits of Figure 3 the vector relationship is in Figure 4.

The voltage along Z divides into a part along the resistive part $U_Z R$ and a part along the reactance $U_Z L$ or $U_Z C$, with a phase difference of 90 degrees. The voltages add up as vectors. Voltage along Z is U_Z . This voltage has a different amplitude and is out-of-phase with the current, which is represented by the voltage U_R along the separate resistor R . This phase difference ϕ is positive for inductive and negative for capacitive components.

In practice it is usually not possible to separate the impedance Z into a resistive and a reactive part, unless the two components are connected as a series circuit. There is no way to measure $U_Z L$ or $U_Z C$, but it is possible to measure the amplitude of U_Z and the phase difference to U_R . Of course this can be proved with both signals displayed on an oscilloscope.

Figure 4 is valid at any given point of time. Even if the signal source is an ac current at some frequency, the phase difference as well as the amplitude ratio will stay the same. The actual phases and actual voltages will change along the sine wave of the signal, but the phase difference and amplitude ratios are stable.

Also important is that the current through all these series real and imaginary components is represented by U_R/R and is always the same. Therefore, if $U_Z L$ or $U_Z C$ is known (or calculated from U_Z and ϕ), the reactance itself can be calculated by using Equation (1), but taking into account that the voltages have different phases.

$$\vec{Z} = \frac{\vec{U}_Z}{I_Z} = R \frac{\vec{U}_Z}{U_R} \quad (2)$$

The vector symbol represents that these are currents and voltages with a phase to take into account, as seen in Figure 5. A complex number could also be expressed in Cartesian form.

$$\vec{Z} = \text{Re}\{\vec{Z}\} + j \text{Im}\{\vec{Z}\} = x + j y \quad (3)$$

The j operator represents 90 degrees phase shift away from the real axis. Any complex number Z will be located in the x - y or real-imaginary plane.

Complex numbers can be expressed in polar form (magnitude and phase), as well as Cartesian form.

$$\vec{Z} = |\vec{Z}| e^{j\phi} = |\vec{Z}| (\cos \phi + j \sin \phi) \quad (4)$$

Refer again to Figure 5.

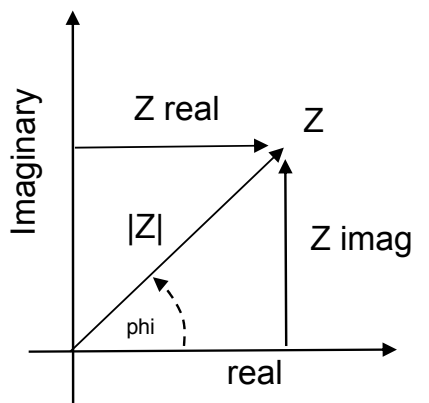


Figure 5 — Vector representation of a complex quantity Z .

The result is that all needed calculations can be done using standard methodologies for complex numbers. Defining the reference phase of U_R to be zero, Equation (2) can be written,

$$\begin{aligned} \bar{Z} &= R \frac{\overline{U_Z}}{\overline{U_R}} = R \frac{|U_Z| e^{j\phi}}{|U_R| e^{j0}} \\ &= \frac{|U_Z|}{|U_R|} (\cos \phi + j \sin \phi) \\ &= \frac{|U_Z|}{|U_R|} \cos \phi + j \frac{|U_Z|}{|U_R|} \sin \phi \end{aligned} \quad (5)$$

The last line of Equation (5) shows how to directly calculate the resistive component and the reactive component of Z if the amplitudes of the voltages and the phase difference between them are known. The set of values is similar to Equation (3), which also shows the form commonly used with network analyzers.

The real and reactive parts carry the units of ohms. By knowing the frequency f of the signal source the capacitance or inductance can be calculated easily,

$$C = \frac{1}{2\pi f X} \quad (6)$$

$$L = \frac{X}{2\pi f} \quad (7)$$

Use Equation (6) when the imaginary part is negative and Equation (7) when it is positive. The missing sign of the imaginary

part of X is the first thing to sort out in antenna analyzers. Analyzers often work just with amplitude ratios and will miss this part of the picture. The IV-Meter does give the sign of X .

The rest of this first part is about how to arrive at a precise measurement of amplitudes (and their ratios) and phase ϕ .

Signal Chain to Measure Impedance

Figure 6 shows a generic block flow diagram of what it takes to measure impedance using handheld instruments. A signal source feeds a signal at the required frequency into a test head. The device under test (antenna, other impedance) is connected to this test head. Depending on the impedance

of the DUT the test head will put out two or more voltages that represent information about amplitudes and phase difference. These voltages will be processed by some analog circuits that are then digitally sampled for further digital processing. The last step is to calculate the target values and present them to the user. A user interface provides the capability to interact with the user (buttons) and provides an underlying layer of control.

One of the key questions that greatly influences cost versus accuracy is where to draw the line between analog and digital processing. The best solution would be to take the RF signals from the test head, directly sample them and do all the rest digitally. For a 100 MHz coverage range that would require a 200 MHz high resolution

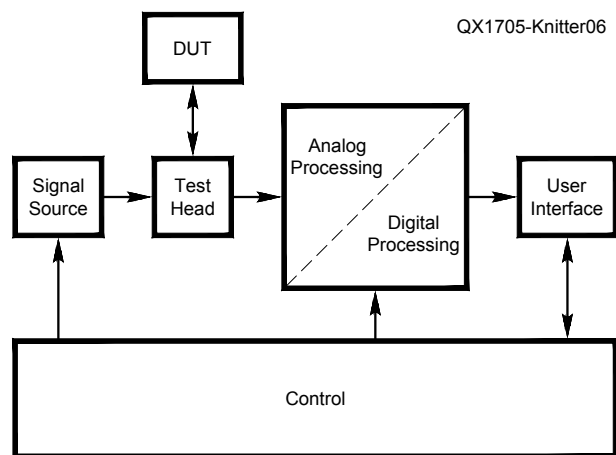


Figure 6 — A generic block flow diagram to measure impedances represented by the DUT.

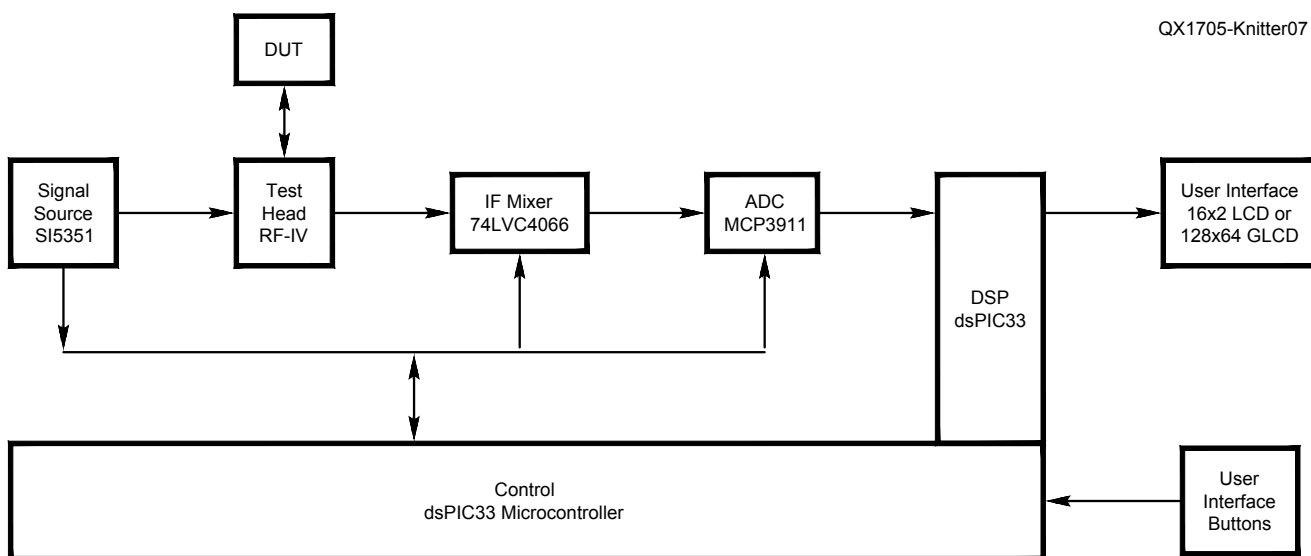


Figure 7 — IV-Meter signal flow and block diagram.

ADC, which would be cost prohibitive. The other extreme would be to do everything analog with peak detectors to get amplitudes and zero-crossing detectors with XOR phase comparison to get a phase difference after integration. That can be done, but it is difficult to handle above a few tens of megahertz, and in the end would deliver medium accuracy at best. Many different concepts can be explored.³ The concept used for the IV-Meter is a compromise to deliver high accuracy at very acceptable cost by using a very different set of components than normally used in antenna analyzers.

Figure 7 shows the implemented concept, which is designed around a single-conversion superheterodyne receiver principle. A Silicon Labs SI5351 serves as the signal source for the test head, the IF mixer, and also for the ADC. An RF-IV test head gives back signals at RF frequency which carry the needed amplitude and phase information. These signals are down-converted in parallel to IF (1 kHz) by a large signal mixer built with the 74LVC4066 analog switch.

During conversion, phase difference and amplitude ratio stay the same. With respect to Equation (5), only the ratio is important, not the total value of the amplitudes.

The IF signals are sampled by a Microchip dual 24-bit ADC and passed to a small digital signal processor, again from Microchip, the dsPIC33FJ128. After some DSP magic the phase and amplitude information is used to calculate the unknown impedance values.

The dsPIC chip has enough power to also do all the control, communication and presentation in the system. In the base version, a 2 by 16 character standard display is used while in the planned future version a 128 × 64 dot matrix display will be used to provide more convenience and additional features. For user input, just three buttons are used to keep cost low.

The next paragraphs will discuss each building block in detail along the signal flow, give comparisons on alternative approaches and finally will provide the math for parts of the overall transfer function of the system.

Signal Source

The signal source must provide a stable test signal with a high enough amplitude level on a specific frequency. The target frequency should be selectable down to a one hertz accuracy. Analog oscillators mostly do not meet these requirements and therefore are not discussed here.

The antenna analyzer standard is to use DDS chips from Analog Devices. They are capable of generating an excellent sinusoidal signal but have two key disadvantages for this project. First is cost and the second is power consumption. Have you ever

wondered why many antenna analyzers have 6 to 12 type AA batteries, or a block of rechargeable batteries? A DDS chip easily consumes 50 – 100 mA and often two DDS chips are needed.

The other group of oscillators is programmable crystal oscillators (XOs) like the very good Silicon Labs SI570 used in many SDR radio designs. Unfortunately, again high cost and high power consumption do prevent usage in this project.

A new Amateur Radio “star” was released by Silicon Labs, the SI5341, a crystal-based programmable CMOS multi-clock generator. The target design for this chip is to replace multiple crystal oscillators in televisions, set top boxes and other consumer products. Therefore, it is priced very affordably. Its key advantage in a handheld device is very little power/current consumption. With three outputs enabled it draws just 35 mA.

This device is flexible to configure. It is possible to generate a mixer LO signal that is phase locked to the DUT signal by using the same internal PLL.

But the test signal is a square wave signal. Does this create mixed signals full of distortions and unwanted frequency components? The answer is yes and no. It does create a lot of signal components which are not of interest. Later, it will be shown that they can easily be sorted out by DSP filtering. As long as the DUT (antenna) is a linear system, there will not be any issue. Linear means it does not distort a signal in any other way than changing amplitude or phase at a given frequency. As the output power is just a few milliwatts the assumption of a linear system is true.

Long ago Joseph Fourier showed that any periodic signal can be represented by a superposition of sine signals with different frequencies, amplitudes and phases. A square wave is no different. If the DUT changes any of these superpositioned sine signals just by amplitude and phase there will be no trouble. The set of frequencies will stay the same, a base frequency and harmonics. Due to changed amplitudes and phases, the signal may look completely different, but the frequencies are the same.

The important result is that the base frequency of our square wave signal will behave with the DUT just like a sine, with an amplitude and phase-changed base frequency. There will be an effect on the harmonics, but for the moment they are not of any interest.

To drive this to the extreme, a noise signal is nothing more than all frequencies at the same time in a wide band. With a spectrum analyzer attached to a test head it will be possible to see the changed frequencies simultaneously.

Mathematically, a square wave signal with the amplitude A_0 and base frequency f can be expressed as superpositioned sine or cosine signals according to the Fourier transforms. We use radian frequency, $\omega=2\pi f$. The SI5351 gives a unipolar signal between ground and positive power A_0 ,

$$s(\omega t + \varphi_1) = \frac{A_0}{2} + \frac{2A_0}{\pi} \left(\frac{\cos(\omega t + \varphi_1) - \cos(3\omega t + \varphi_2)}{3} + \frac{\cos(5\omega t + \varphi_3)}{5} \dots \right)$$

that can be written in the form,

$$s(\omega t + \varphi_1) = \frac{A_0}{2} + \frac{2A_0}{\pi} \sum_{k=1}^{\infty} \frac{(-1)^{k-1}}{2k-1} \cos((2k-1)\omega t + \varphi_k) \quad (8)$$

Equation (8) will be needed later, in the mixer and DSP sections, to see how the harmonics are filtered out.

The Test Head

The signal from the signal source flows into the test head attached to the DUT to give measured voltages that carry information about the impedance of the DUT. *The test head might be the most important part of the overall design.* Directional couplers, resistive bridges, test heads based on transformers and coax lines are examples of circuits used in measurements with antenna, network analyzers and SWR meters. There is, however, a lot of confusion on how they function. For network analyzer bridges as well as directional couplers used in SWR meters, most sources talk about circuits that separate the forward travelling wave from the backward travelling wave in the case of mismatched loads.

All that these circuits are doing is taking a sample of the voltage and of the current at one point of the transmission line. They take the samples on the super-positioned wave which is actually a standing wave. From these two complex values (or, amplitude and phase of each), everything else can be calculated mathematically, as long as there are two super ADCs taking these samples with unlimited resolution. SWR, reflection coefficients, loss ratio and, of course, the impedance can be calculated.

We know that the current of the forward wave goes from source to load, and the current from the backward wave goes from load to source. Both voltages add up to the standing wave, so it is possible

to mathematically combine the sampled information (vector algebra) to show two results which represent the different waves. The waves themselves are not split. One of the best explanations of this concept is by Bruene in his 1959 *QST* article.⁴

It does indeed matter how these samples are measured and how the samples are further processed both in analog hardware and mathematically. Depending on what kind of values are needed, one configuration of measurement makes more sense than another configuration of measurement to get acceptable accuracy.

With this in mind, three different types of test heads are evaluated for the IV-Meter: a resistive bridge (Figure 8 top), a resistor based IV head (center), and a transformer based IV head (bottom). For practical measurement, the DUT impedance must be referenced to ground. The point of measurement is shown for each of the three scenarios. On the bridge, the voltage U_1 between the two arms and the total signal voltage U_2 are measured. On the

resistor IV model, the total voltage U_2 and the voltage U_1 across Z are measured. On the transformer model, the transformer acts as a current sensor and generates a voltage U_2 which is proportional to the current through Z and also the voltage U_1 across Z are measured.

Obviously the three scenarios can be mathematically transformed into each other. However, it is important to realize that such mathematical manipulations do not change the accuracy of the measured voltages. Therefore, it is important to use the setup that gives the potentially highest accuracy in terms of measured voltage for a target environment. For a network analyzer, the highest accuracy should be around the reference impedance Z_0 (target environment), and for an IV-Meter the accuracy should be acceptable over a wider range of DUT impedances Z , not just Z_0 .

How can Z be calculated and what is the change to voltages U_1 and U_2 (or their ratio) on different impedances keeping in mind that all values are complex numbers? Using standard voltage divider mathematics, Z and the ratio of U_2 to U_1 for the bridge circuit is,

$$\bar{Z} = 50 \frac{2 + \frac{\bar{U}_2}{U_1}}{\frac{\bar{U}_2}{U_1} - 2} \quad (9)$$

$$\frac{\bar{U}_2}{U_1} = 2 \frac{\bar{Z} + 50}{\bar{Z} - 50} \quad (10)$$

Having amplitudes of U_1 and U_2 and the phase difference between these voltages, Z can be calculated by mathematics using complex numbers. For the resistor IV head, the current is probed indirectly by measuring the total voltage U_2 , according to the following equations,

$$\bar{Z} = \frac{50}{1 - \frac{\bar{U}_2}{U_1}} = 50 \frac{\bar{U}_1}{U_1 - \bar{U}_2} \quad (11)$$

$$\frac{\bar{U}_2}{U_1} = \frac{\bar{Z}}{\bar{Z} + 50} \quad (12)$$

Finally, the IV transformer head leads to the following equations with a constant c introduced by choosing a specific transformer winding ratio with attached resistor.

$$\bar{Z} = c \frac{\bar{U}_1}{U_2} \quad (13)$$

$$\frac{\bar{U}_1}{U_2} = \frac{\bar{Z}}{c} \quad (14)$$

It gets interesting if Equations (10), (12), and (14) are plotted against the real parts of Z , see Figure 9. For the bridge head there are large changes in amplitude ratio around $Z = 50 \Omega$. That means that any measurement is probably very accurate around 50Ω . The downside is the change in voltage ratio gets smaller as the impedance differs from 50Ω . In addition, whatever is used to measure these voltages needs to have a very large dynamic range. Practically, most antenna analyzers⁵ will exhibit large inaccuracy for a few hundred ohms because of this.

The resistor IV head shows medium ratio changes in the low impedance area and very flat ratios at higher impedances. What might be a disadvantage for analog circuits to measure, may look different on mixers followed by high resolution ADCs. The signals will stay on a relative high voltage level with a high signal-to-noise ratio (SNR). Little dynamic range is needed, but instead,

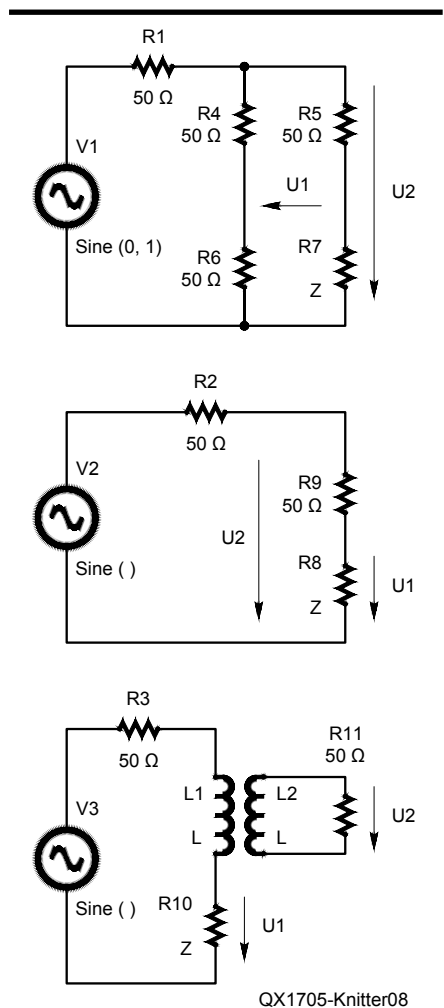


Figure 8 — A resistive bridge (top), resistor IV head (center), transformer IV head (bottom).

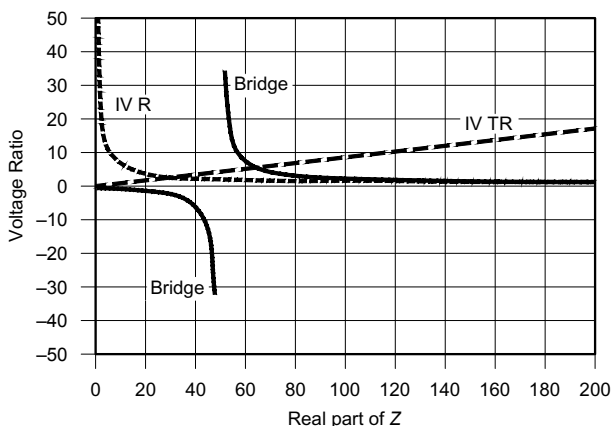


Figure 9 — Voltage ratios for different test heads plotted against the real parts of Z .

a high resolution is required. Finally, the transformer based IV head shows a true linear ratio. Medium dynamic range will likely lead to the same accuracy along Z. For wide coverage IV-Meters this is the ideal scenario.

A lot of tests and measurements were done on all three test head configurations. Transformer based solutions in hand held instruments showed too much sensitivity to unwanted stray capacitance coupling to the user, unless there is extensive shielding of the transformer. Differential mixers to measure voltages directly on components not attached to ground, were either too expensive or had other limitations. For example, the popular NE612 works only on very low amplitudes.

Instead, a mix of the bridge (hardware) and the resistor-based RF head (measurement) emerged as the best combination with the selected mixer and ADC, and produced the highest accuracy of all three combinations in an impedance range from 5 to 1000 Ω .

The final version of the IV-Meter measures the voltages across the DUT Z, and across the equivalent resistor in the second arm of the bridge, R6 in Figure 8 (top). The resulting voltage ratio looks similar to the plot from the IV head in Figure 9, as the voltage along R6 is simply half of U_2 . All following discussions will therefore use this IV head model.

Using a bridge design has the advantage of a symmetry for both of the measured voltages at $Z = Z_0$. This will cancel out some unwanted influences in the mixer section.

Two other areas are taken into account. First, the test head should have an output impedance of 50 Ω . This will avoid additional reflected waves if cables with the same impedance are attached to the analyzer for measurement. Second, the test head must be designed so that the voltages stay in a specific range for all impedances. If the voltage is too high, a mixer or ADC may overload, if the voltage is too low, noise is introduced. This is why the final test head has resistors for scaling of the measured signals and for impedance matching.

The Mixer

The test head delivers two voltages to the mixer. As in a software defined radio, the goal is to sample the signals to the digital domain as early as possible. Because of the cost of ADCs this cannot be done directly at the RF frequency.

A mixer is used to heterodyne down the RF frequency to an intermediate frequency, or even down to base band. The important thing is that mixing will not change the ratio of the voltages nor their phase difference.

If there is one driver for not doing baseband mixing and for not choosing the popular NE612 as a mixer, it is the physical layout of the IV-Meter. Compared to other

designs it is very compact, the display will cross test head and mixer section. The microcontroller and the SI5351 produce a lot of noise — up to 40 mV — on the power supply lines. All this leads to a generally high level signal design with IF mixing, which is insensitive to medium levels of noise.

The NE612 is popular, but it is designed for low level signals. Above 6 mV signal level it gets very non-linear in terms of amplitude. All signals need to be scaled down. Baseband mixing will produce voltages to be sampled of just a few millivolts. This would be a very big challenge in a compact system with noise.

The solution was to use a large-signal mixer, the 74LVC4066. It can easily cover oscillator frequencies up to 100 MHz at low cost and can work at an operating point of half the supply voltage. Moreover it has a very low on-resistance and has linear amplitude response around the operating point.

An IF frequency of 1 kHz was chosen for practical reasons. This is low enough to allow large oversampling by the ADC, and high enough to use small values of coupling capacitors.

The SI5351 will deliver both the test signal, modified by the test head and DUT, and the local oscillator signal to the mixer. Both are square waves. Mixing two square waves is mathematically meaningful, as we will show.

Fourier is Our Friend

Equation (8) shows the square wave signal from the SI5351, which serves as the signal source. This signal is applied to the test head and will be changed by the DUT in amplitude and phase for the base frequency as well as for the harmonics. There are two signals from the test head, but they are mixed separately in parallel. What works for one signal, it will work for the other.

The mixer is ac-coupled with an operating point of half the supply voltage U_b so the input signal to the mixer will be,

$$u(\omega_s t) = \frac{U_b}{2} + \frac{2A_0}{\pi} \left(\begin{array}{l} c_1 \cos(\omega_s t + \varphi_{u1}) \\ - \frac{c_2 \cos(3\omega_s t + \varphi_{u2})}{3} \\ + \frac{c_3 \cos(5\omega_s t + \varphi_{u3})}{5} \dots \end{array} \right) \quad (15)$$

Each frequency has a different phase φ and a different coefficient $c < 1$. The phase and amplitude changes in the test head for each frequency are unknowns.

Turning an analog switch on and off is nothing more than multiplying the signal with a unipolar square wave of amplitude one. Doing this with the local oscillator frequency ω_0 this square wave can be expressed as,

$$v(\omega_0 t) = \frac{U_b}{2} + \frac{2}{\pi} \left(\begin{array}{l} \cos(\omega_0 t + \varphi_{L1}) \\ - \frac{\cos(3\omega_0 t + \varphi_{L2})}{3} \\ + \frac{\cos(5\omega_0 t + \varphi_{L3})}{5} \dots \end{array} \right) \quad (16)$$

The multiplication of signals at two frequencies results in signals at the sum and difference frequencies. So multiplying the signals u of Equations (15) and v of (16) will result in signals at frequencies $(m\omega_s + n\omega_0)$ and $(m\omega_s - n\omega_0)$ for all integers m and n greater than zero. Except for the terms where $m = n$, all other components are at multiples of the RF frequency and can be removed by low pass filtering. The terms where $m = n$ that are at multiples of the RF frequency can also be removed by low pass filtering. How to best low-pass filter these signals will be covered in the next section. The dc terms will be blocked by ac coupling. That leaves,

$$uv = \frac{2A_0}{\pi^2} \left[\begin{array}{l} c_1 \cos((\omega_s - \omega_0)t + \varphi_{u1} - \varphi_{L1}) \\ + \frac{c_2 \cos((3\omega_s - 3\omega_0)t + \varphi_{u2} - \varphi_{L2})}{3^2} \\ + \dots \end{array} \right] \quad (17)$$

that can be expressed as,

$$uv = \frac{2A_0}{\pi^2} \sum_{k=1}^{\infty} \frac{c_k \cos((2k-1)(\omega_s - \omega_0)t + \varphi_{uk} - \varphi_{Lk})}{(2k-1)^2}$$

If the signal frequency and the local oscillator frequency differ by the IF (here 1 kHz) the resulting signal consists of components of multiples of the IF frequency (1 kHz, 3 kHz, 5 kHz...). With a DSP it is quiet easy to separate the 1 kHz signal from the rest. The result is a 1 kHz signal that includes the phase difference as well as an amplitude information from just the base frequency components of the incoming signals. This is a very remarkable result. With some filtering, mixing two square waves can be used instead of mixing two sine waves or a sine wave with a square wave.

More than that, selecting the 3 kHz term by DSP band pass filtering results in the phase difference and amplitude information of the 3rd harmonic of the incoming signals. For an

antenna analyzer that means the impedance at the 3rd harmonic frequency can be observed simply by changing the DSP filtering to take a look at a different IF frequency. The only limitation is the bandwidth of the mixer and the signal chain. If this were designed for multiple hundreds of megahertz, it would be possible to measure the impedance at such high frequencies. This is definitely something worth considering at a future date.

If signal frequency and local oscillator frequency are the same, the mixing results in baseband, but information from base frequency and harmonics are overlaid. That will not work with two square waves.

Equation (17) includes constants c_k , which were introduced to handle different amplitude changes on base frequency and harmonics. If the load Z is real, for example 50Ω these constants will all be one. In that case Equation (17) is the Fourier Transform of a triangular wave. Figure 10 shows an oscilloscope plot of the IF signal right after the anti-aliasing filter, but before the ADC, with an attached 50Ω load to the IV-Meter for RF at 10 MHz.

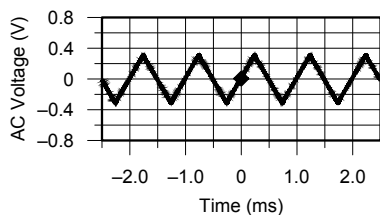
To complete the picture, this mixing process applies in parallel with the second signal from the test head. All the needed information is available to get processed and mathematically manipulated to show the impedance and SWR of the DUT.

The ADC

The next step in the signal chain is sampling the two signals from the test head. All the rest of the processing can be done in the software of the microcontroller/digital signal processor.

The required ADC works on two channels in parallel with sufficient resolution. Speed is less critical, because only low frequencies are involved. The target low frequency measurement range of the IV-Meter is 100 kHz or less. But, it cannot be too low, to avoid difficulties in building analog anti-aliasing filters.

Other requirements of the ADC are low power consumption, easy-to-use analog input stages, not too low impedance, an input signal level relative to ground, as well



QX1705-Knitter10

Figure 10 — An IF signal with 50Ω load after low pass filter, but before the ADC.

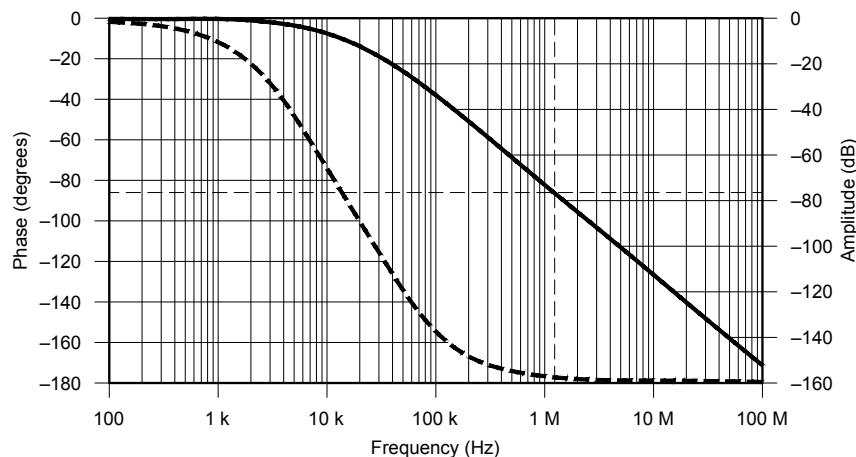
as standard interfaces to the microcontroller. There are great solutions available that fulfill all these requirements, but most are rather expensive for Amateur Radio hobbyists.

The MCP3911 from Microchip turned out to be an ideal low cost candidate. It is designed to work as an analog front end in power meters, but actually it is a full scale two channel 24-bit ADC, that is extensively configurable. It consumes less than 10 mW, so a 1 kHz signal can easily be sampled at 2.5 MHz (1250 times oversampling) to deliver decimated 24-bit data via a standard SPI interface at 20 MHz. The ADC analog inputs allow ± 600 mV against ground, which makes ac coupling extremely easy.

The high oversampling rate combined

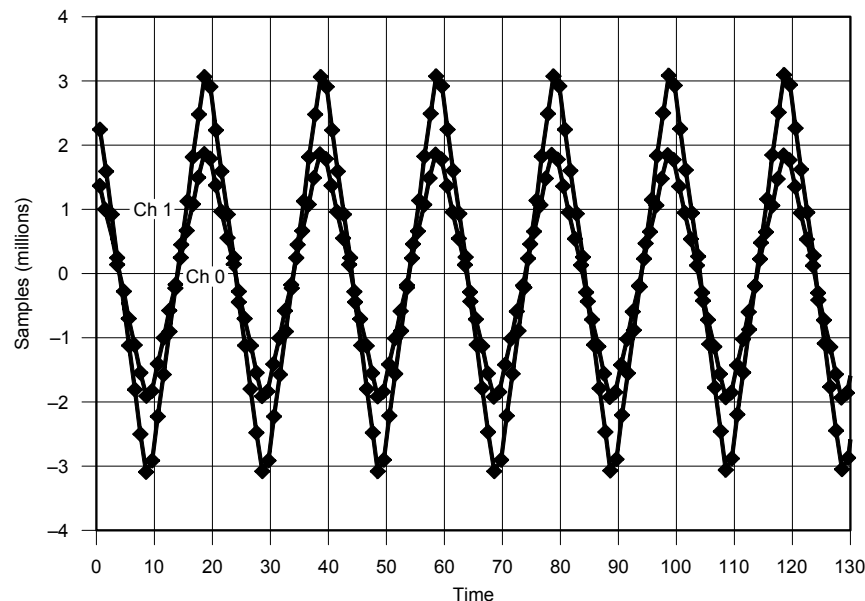
with a high input impedance of more than $200 \text{ k}\Omega$ allows for a very straight forward anti-aliasing filter design. LF and RF signals up to 1.25 MHz can be sampled directly. Everything above that should be attenuated to a level that does not affect further processing.

A cascade of two RC low pass filters is sufficient. Figure 11 shows a LTSpice simulation of this filter. At an IF frequency of 1 kHz the attenuation is just 0.2 dB. At 1.25 MHz it is 76.6 dB. This makes a good fit to the resolution of a 16-bit ADC. The net dynamic bandwidth of the IV-Meter signal chain is not higher than 76.6 dB. Realistically, even 80 dB would be very challenging for a compact hand held device. To visualize the result of the sampling process, Figure 12 was



QX1705-Knitter11

Figure 11 — Transfer function of a cascade of two RC low-pass anti-aliasing filters.



QX1705-Knitter12

Figure 12 — Samples of the IF signal from Figure 10.

captured from the microcontroller memory, and exported to a signal graph via an Excel spreadsheet.

DSP and Mathematics

The next step is to select a microcontroller and / or digital signal processor. It must be cost efficient, consume acceptable power, have SPI and other interfaces, and must be powerful enough to do basic digital signal processing. The Microchip dsPIC 16-bit series fulfills all those requirements. It also includes a fixed point DSP kernel, and is supported by extensive DSP libraries. The dsPIC includes two fast 12-bit ADCs as well, but they are of insufficient accuracy for use here.

Equation (11) shows how to calculate Z from the two voltage signals U_1 and U_2 that carry the components outlined in Equation (17). Assuming there is no relevant aliasing during the sampling process, formulas for continuous signals can be used instead of formulas for discrete samples. With help of Equation (5) and moving the 50 Ω resistor to general resistor R , Equation (11) becomes,

$$\begin{aligned} \bar{Z} &= R \frac{\overline{U_1}}{\overline{U_1 - U_2}} = R \frac{\overline{U_1}}{\overline{U_{12}}} \\ &= R \frac{|U_1|}{|U_{12}|} \cos \Delta\phi + j R \frac{|U_1|}{|U_{12}|} \sin \Delta\phi \end{aligned} \quad (18)$$

This means the ratio of the amplitudes of U_1 and the difference $U_{12} = U_1 - U_2$ as well as the phase difference of these two signals is needed to arrive at the resistive and reactive part of Z .

Z can also be calculated without using the difference of $U_1 - U_2$, but the formulas will become more complex. The described usage of the bridge hardware with additional scaling and impedance matching will add additional complexity to the formulas, without changing the principle method. In the end it is always about using the ratio of the measured amplitudes and the phase difference between the signals. To keep the mathematics lean, Equation (18) will be the basis for further explanations.

To complete the picture, having Z in a system with Z_0 (usually 50 Ω) will allow us to calculate the reflection coefficient Γ and the SWR using standard complex arithmetic,

$$\bar{\Gamma} = \frac{\bar{Z} - Z_0}{\bar{Z} + Z_0} \quad (19)$$

$$SWR = \frac{1 + |\bar{\Gamma}|}{1 - |\bar{\Gamma}|} \quad (20)$$

To get the amplitudes or absolute values for two signals and also their phase difference requires more mathematics. First the two signals from the ADC, Equation (17), must be filtered to contain only the target component of the IF frequency. Next, 90-degree phase shifted versions of the signals will be needed. These four signals are called in-phase and quadrature signals u_{1i} , u_{1q} , u_{2i} , and u_{2q} .

With a DSP, filtering and shifting can be done with just one FIR filter. A 64-tap phase added band pass filter is used to create the four signals from the two original ones. Component u_{1q} is 90-degree phase shifted with respect to u_{1i} , and u_{2q} is 90-degree phase shifted with respect to u_{2i} . This 90-degree shift is called a Hilbert transform.

An FIR filter does nothing else than take a row of input samples, multiply each of the FIR samples with a different coefficient, and add up all the products to form one new output sample. For the next output sample this multiplication and accumulation machine is shifted one sample on the input samples. The different coefficients are also called the kernels of the filter. A 64-tap FIR filter therefore has 64 coefficients. Software⁶ can be used to calculate the coefficients by interactively designing the transfer function of the filter. See the Guide to DSP⁷ for an excellent source about DSP. Figure 13 shows the transfer function of the DSP filter. The next, unwanted signal at 3 kHz is attenuated by more than 80 dB.

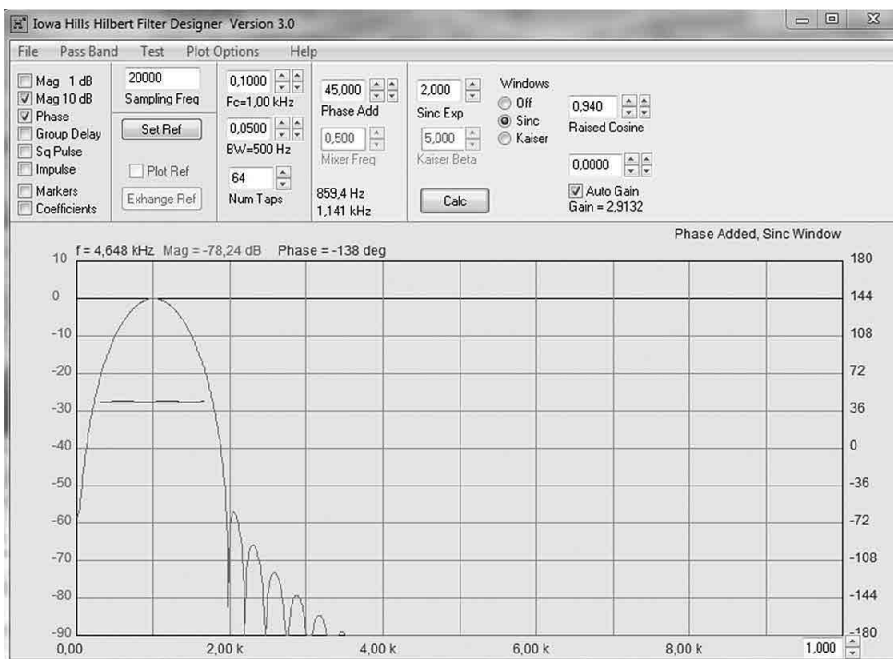


Figure 13 — The transfer function of the amplitude and phase of the DSP filter.

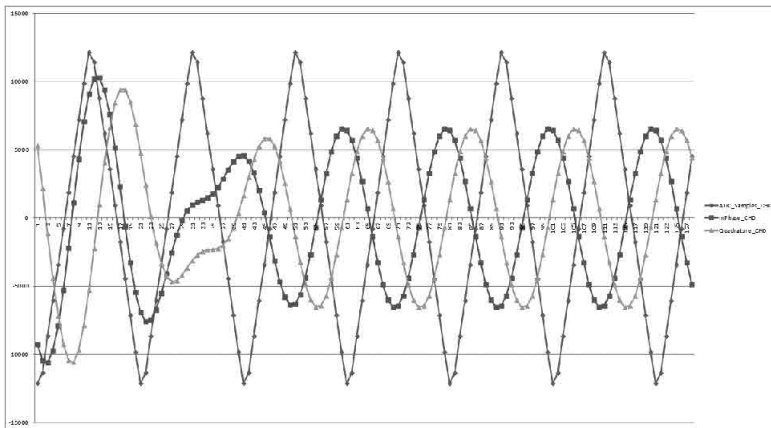


Figure 14 — The triangular IF signal, and the filtered and shifted in-phase and quadrature signals.

Since an FIR filter adds delay, the easiest way to keep all the signals in synch is to take an original signal and create two new ones. One signal is band-pass filtered and shifted +45 degrees, the other one band-pass filtered and shifted -45 degrees. The result is two new signals in quadrature, both delayed by the same amount.

Figure 14 shows the result of this DSP activity, again taken as a memory dump and visualized using an Excel spreadsheet plot. The triangular signal (tallest) is the input to the filter, the two sine curves are the band-pass filtered in-phase and quadrature components. It is nice to see how the shift works on the first 64 samples. This also makes clear that the first 64 samples cannot be used for further processing. They are truncated and the remaining samples (here another 64 samples) are taken for further processing.

Now it also becomes clear why first filtering and shifting is applied, then afterwards the difference $U_1 - U_2$ is built. Using fixed-point DSP, unnecessary scaling is avoided and the filter can operate at high level input signals. Taking the difference $U_d = U_1 - U_2$ results in four signals for further processing arriving from the filtered signal, Equation (17). Coefficient c_2 and φ are a constant and a phase angle of the difference of the two signals,

$$u_{1I}(\omega_{if}t) = \frac{2A_0}{\pi^2} c_1 \cos(\omega_{if}t + \varphi_1) \quad (21)$$

$$u_{1Q}(\omega_{if}t) = \frac{2A_0}{\pi^2} c_1 \sin(\omega_{if}t + \varphi_1) \quad (22)$$

$$u_{dI}(\omega_{if}t) = \frac{2A_0}{\pi^2} c_2 \cos(\omega_{if}t + \varphi_2) \quad (23)$$

$$u_{dQ}(\omega_{if}t) = \frac{2A_0}{\pi^2} c_2 \sin(\omega_{if}t + \varphi_2) \quad (24)$$

The absolute value of a signal can be calculated by using the in-phase and quadrature signal (Figure 5),

$$|u_1| = \sqrt{u_{1I}(\omega_{if}t)^2 + u_{1Q}(\omega_{if}t)^2} \quad (25)$$

$$|u_d| = \sqrt{u_{dI}(\omega_{if}t)^2 + u_{dQ}(\omega_{if}t)^2} \quad (26)$$

The phase difference between the two signals u_1 and u_d does not necessarily stay between a specific range. The methodology must work on full 360 degrees. The standard way to get the phase angle for a complex quantity u_1 , against the real axis, here equivalent to phase signal, is

$$\varphi_1 = \arctan\left(\frac{u_{1Q}(\omega_{if}t)}{u_{1I}(\omega_{if}t)}\right) \quad (27)$$

$$\varphi_d = \arctan\left(\frac{u_{dQ}(\omega_{if}t)}{u_{dI}(\omega_{if}t)}\right) \quad (28)$$

The software computing Equations (27) and (28) is from a math library using the four-quadrant `atan2` function instead of the two-quadrant `atan` function. Note that the vectors u_1 and u_d do not really exist in the system. They are just artificial references for calculating phases for the existing signals u_{1i} , u_{1q} , u_{di} , u_{dq} . The in-phase signals u_{1i} and u_{di} have the same reference phase as the artificial vectors and therefore the phase difference is the same.

$$|\varphi_1 - \varphi_d| \leq \pi : \delta\varphi = \varphi_1 - \varphi_d \quad (29)$$

$$(\varphi_1 - \varphi_d) > \pi : \delta\varphi = -2\pi + \varphi_1 - \varphi_d \quad (30)$$

$$(\varphi_1 - \varphi_d) < -\pi : \delta\varphi = 2\pi + \varphi_1 - \varphi_d \quad (31)$$

Equation (29) will work except for one special case. Figure 15 (top) helps to illustrate the concept. The phase differences are periodic, which means that phase can run between 0 and 2π and then jump back to 0. This creates trouble if one vector has crossed this point and the other one has not. The net result is that the opposite phase difference of the two vectors will be calculated. Figure 15 (bottom) shows this situation.

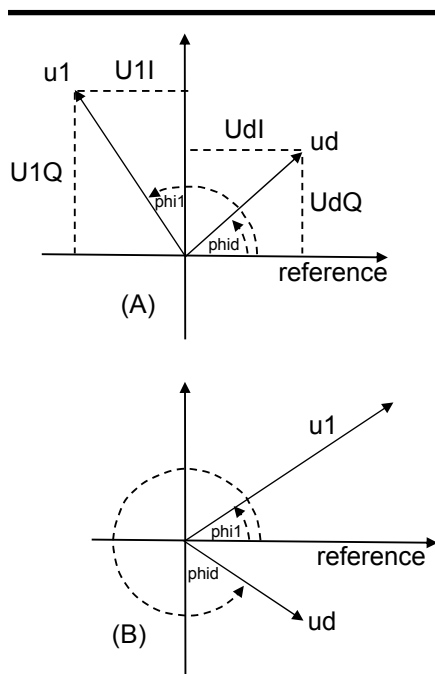


Figure 15 — Phase difference between two signals.

The mathematical solution is to check if the absolute value of the phase difference is greater than π and use Equations (30) and (31) for calculating the difference.

In summary, use Equations (25) and (26) for the amplitudes of the signals from the test head, and Equations (29) to (31) for the phase difference between the signals. Then calculate Z from Equation (5) and SWR from Equations (19) and (20).

Just the kernel length plus one are enough samples to get a meaningful value. In reality more samples will be calculated and averaged to smooth the values since noise and other distortions are in the system.

Short-Open-Load (SOL) Compensation

Whenever a connector is attached to the antenna analyzer, the cable used will change the measurement due to parasitic capacitance, inductance and resistance. More than that, ham radio operators know that cable lengths can change impedance measurements due to the added phase length and cable losses. The IV-Meter uses short, open, load (SOL) compensation to resolve these issues. The operator need not take the analyzer to the top of an antenna tower and attach it directly to the antenna connector. Instead, any cable can be used. Attach one end to the IV-Meter, the other end to be connected sequentially to a short, an open and defined load standard. After that, the cable can be attached to the antenna and the measurement can be done from the other side of the cable in the ham shack.

This compensation technique is standard for professional instruments and all network analyzers, see Note 1. Compensation models the connector and cable and everything else as an unknown 4-port network. By using reference short, open and load standards, the cable is merged into the meter circuit, and the measurement is as if this unknown network did not exist. For the HF range the SOL standards are very easy to build inexpensively. Figure 16 shows simple BNC-connector standards, the 50 Ω standard is built from a leaded resistor. The right side of the Figure shows professional SMA standards.

The IV-Meter stores the SOL compensation values for the full coverage range, but also allows a quick compensation on a specific frequency. This gives maximum flexibility to the operator.

Putting It All Together – The DG5MK IV-Meter Implementation

The IV-Meter schematic, bill of material, board layout and implementation details (and software) are on the *QEXfiles* web page.⁸

The PCB fits into a TB-2B enclosure

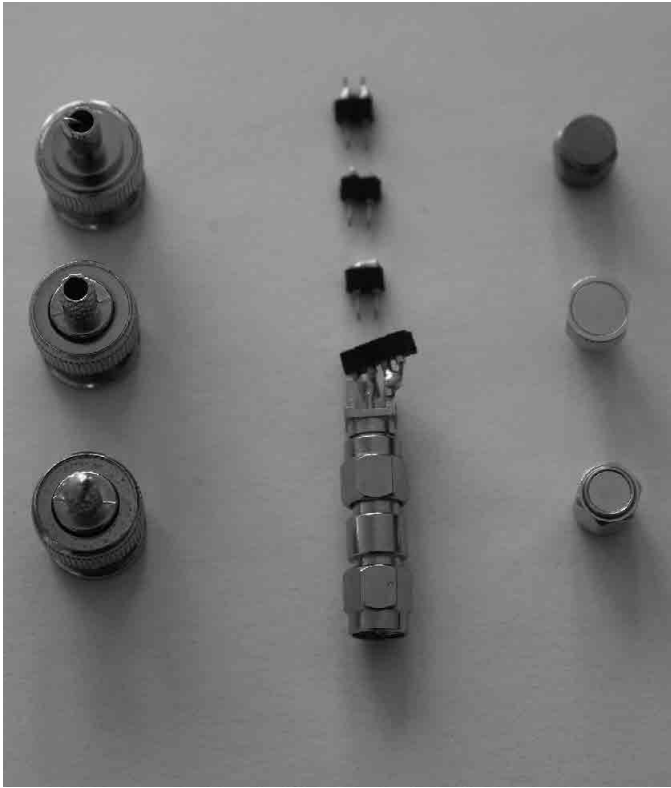


Figure 16 — Short-Open-Load (SOL) standards.

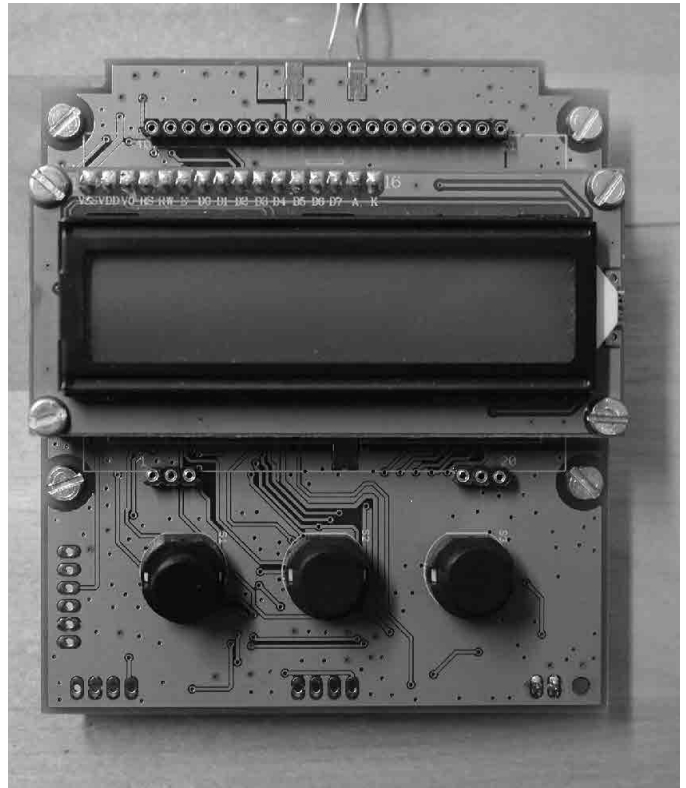


Figure 17 — Front face of PCB.

from TEKO. In general, the PCB leaves ample free space, so there is room to install either SMA or BNC, or N-type or UHF-type connectors at the builder's option. Figure 17 shows the LCD and control buttons on the front side of the PCB. Figure 18 shows the back side of the assembled PCB.

The Software

Another complete article could be dedicated to describe the software of the IV-Meter. Some of the challenges include:

[1] – Critical timing of all internal communication between microcontroller and peripherals via SPI bus and I2C bus, also interrupt-driven sample transfer from the ADC to microcontroller.

[2] – Implementation of fixed point DSP filters.

[3] – State machine design to keep different operating modes separated and to make the changes for the right modes on menu actions.

[4] – Speed optimization that includes different DSP implementations and dynamic switching of CPU speed.

[5] – Power consumption optimization, which includes dynamic power down of components, dynamic delay routines and CPU speeds.

[6] – Smooth user interaction for display (double buffering), and interrupt driven button activity.

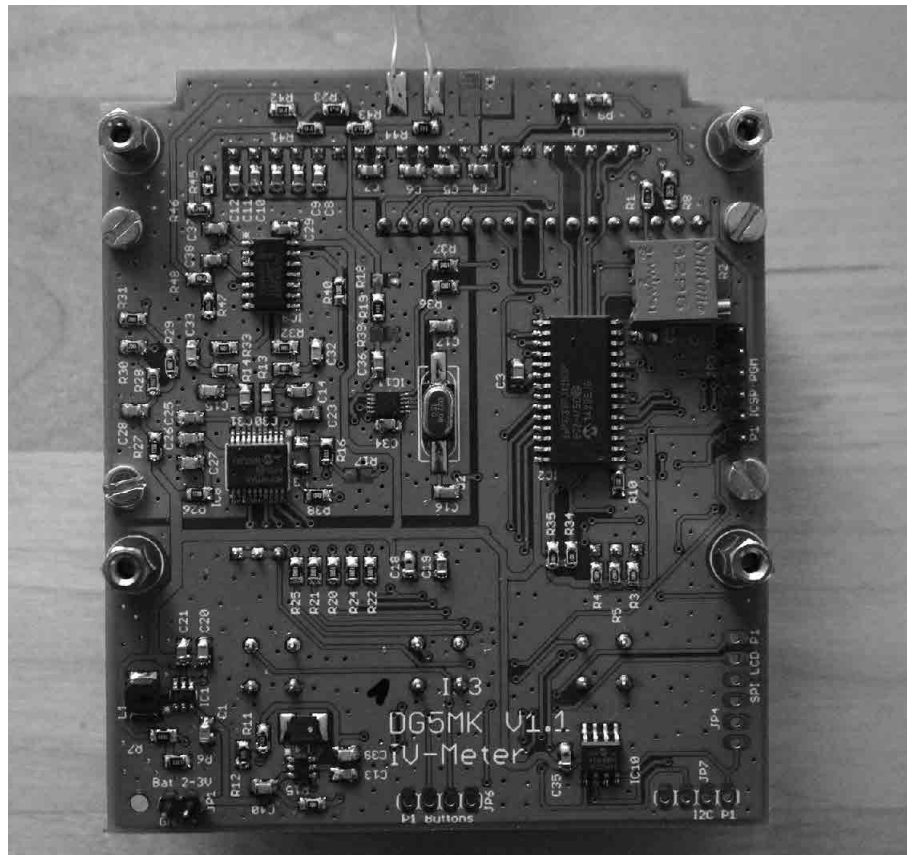


Figure 18 — Back side of PCB.

[7] – Arrive at best fit for largely different configuration scenarios in terms of IF, sample rates, DSP filters and mathematical accuracy, in balance with power consumption, speed, user experience and final accuracy.

Everything is programmed in C using the Microchip MPLAB IDE development environment. The program fills just 20 % of the program memory, so cost can be optimized by using a microcontroller with a smaller flash memory. The software is included on the *QEXfiles* web page.

Functionality of the IV-Meter

In addition to the LCD contrast potentiometer there are only three buttons to control the IV-Meter: left, middle and right. Usage is very intuitive.

These buttons have different meanings depending on which mode the IV-Meter is in. But generally pressing the left button for a *long* period switches over to a menu that allows further selection. *Short* pressing the left button toggles through the different options, pressing the right button selects the option. Table 1 describes the Menu Modes.

The IV-Meter has just two actual modes, the *SWR/Z* measurement and a frequency generator. When the signal is switched off after the *SWR/Z* measurement there is the second mode to produce a steady signal.

The “SOL current” frequency compensation is valid just for the present frequency and will automatically switch over to “SOL all” frequencies if frequency is changed. The letters “SOL” in the display show usage of “SOL current” frequency compensation.

If the option “SOL current” frequency is selected the operator is asked to connect a short, an open, and a load standard (50 Ω) as guided by the menu, and confirmed by pressing the right button. “SOL all” frequencies works the same way, and will take several minutes as the device runs through all frequencies and stores the parameters into the EEPROM for every 100 kHz.

The idea is to enable the operator to compensate one time with “SOL all” frequencies depending on which connector or cable is used most often. For actual measurements it is recommended to perform a quick “SOL current” frequency compensation to take any current changes into account. The “SOL current” frequency is performed with higher internal accuracy.

In both “Measure *SWR/Z*” and “f-Generator” mode the left button is used to switch from frequency to frequency digit. The middle and right buttons are used to increase or decrease the measurement frequency.

In “Measure *SWR/Z*” mode the display

Table 1

<i>Menu mode</i>	<i>Action</i>
Return	Returns to normal operating mode
Measure <i>SWR/Z</i>	<i>SWR/Z</i> measurement with cycling updates
f-Generator	Frequency generator with steady signal
SOL current	Perform short, open, load calibration for current frequency
SOL all	Perform short, open, load calibration for all frequencies
Setup	Further options as shown below.

Table 2

<i>Setup mode</i>	<i>Action</i>
Return	Returns to normal operating mode
Update Cycle	Change cycle to slow, medium, fast
Backlight	Change backlight to off, on, auto
Display Data	Select <i>SWR</i> or capacitance/inductance to be displayed
Delta Frequency	Calibrate crystal frequency
Reset Configuration	Reset all EEPROM data to default.

Table 3

Performance of the IV-Meter, PCB Version 1.1, SW Version 0.28b.

<i>Parameter:</i>	<i>Value</i>
Measurement range	100 kHz to 100 MHz, 1 Hz steps
<i>SWR</i> range	1:1 to at least 1:100
Z range	To at least 1000 Ω
Sign of X	Yes
Accuracy	100 kHz to 50 MHz better than 2% for Z smaller than 1000 Ω
Battery	Two 1.5 V AA, or two 1.2 V rechargeable cells
Socket	SMA (or BNC, N-type, UHF-type)
Output power	square wave 0.5 Veff, 7 dBm, 100 kHz to 100 MHz
Power requirements	Internal 3.0 V, average 49 mA, peak 110 mA at 100 MHz, 50 Ω load, backlight off
Size	175 mm by 95 mm by 25 mm (TB-2B enclosure)
Weight	270 g including. two 1.2 V NiMH battery.

will always show the measurement frequency in kilohertz, complex Z and either the *SWR* or the capacitance/inductance. The latter depends on an option selected in setup.

The frequency in *SWR/Z* mode can be adjusted to a 1 Hz resolution as well by doing this in f-Generator mode and switching over to Measure *SWR/Z* mode.

The Setup Mode options are described in Table 2. On every item of the setup menu the left button will toggle through the options and right button will select the action. In the following submenus the usage is similar and intuitive.

The “Backlight” auto option switches backlight on with every interaction and off after a few cycles to save power.

“Delta Frequency” is an option to calibrate the internal frequency reference. A 27 MHz crystal is used for generating all clocks. The adjustment is simple. After attaching a calibrated frequency counter to the output the “Delta Frequency” is increased or decreased until the output frequency matches the calibrated counter frequency.

All settings are stored in the EEPROM and will stay after power off. “Reset Configuration” will change all settings to factory default, but the “SOL all” frequency values will stay until they are overwritten by new values.

Practical Measurements

The IV-Meter can be used in any measurement environment where an operator is interested in the complex impedance of a 2-port network at a given frequency. A big feature is to take into account any intervening 4-port network (like a connecting cable) into consideration by SOL compensation.

After complete assembly, including HF connector, the operator should run a “SOL all” frequency compensation. The SOL standards should be attached to the connector directly, or if always used with a cable, at the other end of that cable. The IV-Meter is now ready for rapid measurements.

For antenna *SWR* measurements, the IV-Meter should be attached as close as

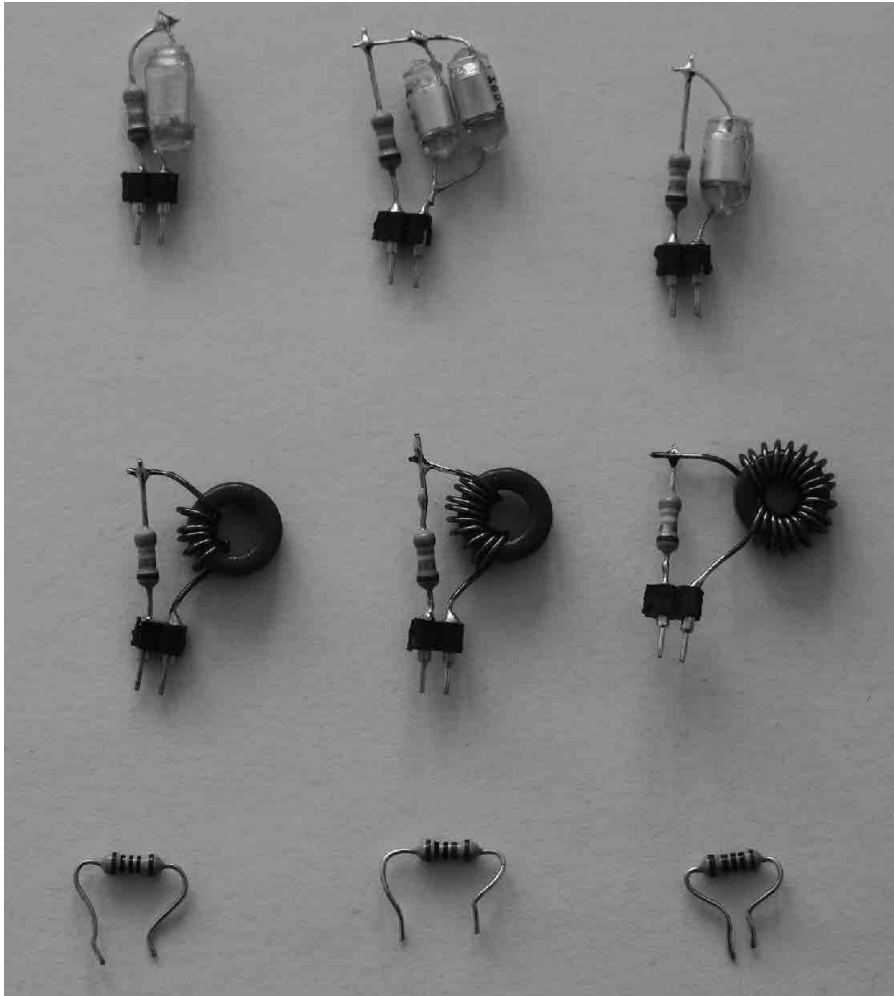


Figure 19 — DUT loads used for accuracy measurements.

possible to the feed point of the antenna. Optionally, or if used with an antenna cable, the IV-Meter should be attached to one side of this cable, perform the “SOL current” frequency compensation on the other side of the cable, and attach the cable afterwards to the feed point of the antenna for measurement.

The IV-Meter can be used to measure inductance or capacitance at any target frequency by just attaching the DUT to the connector. The highest accuracy is achieved if the corresponding measured Z is between ten and a few hundred ohms. An Internet search and manuals from other units give good ideas about what is possible.

Accuracy of the IV-Meter

The ARRL Lab performed comparisons of similar antenna analyzers [see Note 5]. These ‘proof points’ were used to challenge the accuracy of the IV-Meter. Figure 19 shows several DUTs, standard metal film resistors in combination with selected

toroid inductors and Styroflex capacitors, used to align with the ARRL measurement scenarios. These DUTs were measured with a DG8SAQ VNA network analyzer (www.sdr-kits.net) with attached RF-ID measurement head. SOL compensation was performed for each frequency just before the measurement. The details are presented in the *QEXfiles* web page. In most cases the IV-Meter outperforms the other analyzers by far, except for the Agilent 4291B reference used in the reference tests.

The measurements prove that the IV-Meter is a very accurate instrument in the full HF range up to 30 MHz, and is also very usable up to 100 MHz for ham radio needs.

Technical Data of the IV-Meter

The technical data for the IV-Meter, resulting from the sample measurements, is shown in Table 3. Power requirements are very low, so an external supply was omitted. Drawing just 50 mA, the IV-Meter will allow more than 40 hours of measurements from

just one pair of AA alkaline batteries!

The IV-Meter design is based on the SI5351 at 3.3 V with 50 Ω output impedance. The total output impedance of the bridge circuit is also matched to 50 Ω . This limits the output voltage to 500 mV effective across 50 Ω . It is theoretically possible that measurements might be influenced by strong radio stations near the antenna under measurement. On the other hand, the IV-Meter is very selective about the measurement frequency due to the superheterodyne architecture.

Summary

The IV-Meter was developed to provide an affordable, but accurate antenna analyzer available to every ham radio operator who is interested in antenna building and impedance measurements. This could become a nice weekend project for ham radio clubs.

All the needed files, like PCB layout, bill of materials, microcontroller hex code and circuit diagram are available on the *QEXfiles* web page. Please also check the author’s web page for possible updates and announcements.

Michael Knitter, DG5MK, has been a licensed radio amateur since 2006. He earned a degree in telecommunication technology from the University of Dortmund, and works in an international computer company in sales and distribution. He has always been involved with electronics and radio communications. Michael’s special areas of interest are software defined radio, digital signal processing, filter design, magnetic loop antennas, microcontrollers, C++ and Labview programming. He loves to sail as a true contrast to a modern busy life.

Notes

- ¹HP/Agilent/Keysight Network Analyzer Basics, cp.literature.agilent.com/litweb/pdf/5965-7917E.pdf.
- ²A short review of antenna and network analyzers, Rig Expert, www.rigexpert.com/index?s=articles&f=aas.
- ³HP/Agilent/Keysight Impedance Measurement Handbook, cp.literature.agilent.com/litweb/pdf/5950-3000.pdf.
- ⁴Warren B. Bruene, WØTTK, “An Inside Picture of Directional Wattmeters” *QST* Apr 1959, pp 24-28.
- ⁵Joel R. Hallas, W1ZR, “A Look at Four Antenna Analyzers (Comet CAA-500; MFJ-266; RigExpert AA-54; Youkits FG-01) (Product Review)”, *QST* Mar 2012, pp 46-52.
- ⁶Iowa Hills Software, Digital and Analog Filters, www.iowahills.com.
- ⁷Steven W. Smith, “The Scientist and Engineer’s Guide to Digital Signal Processing” www.dspguide.com.
- ⁸www.arrl.org/qexfiles.
- ⁹Author’s web page, www.dg5mk.de.



Showroom Staffing Hours:
9 am to 5 pm, Monday-Saturday

Ordering (via phone):
8:30 am to midnight ET, Monday-Friday
8:30 am to 5 pm ET, Weekends

Phone or e-mail Tech Support: 330-572-3200
8:30 am to 7 pm ET, Monday-Friday
9:00 am to 5 pm ET, Saturday
All Times Eastern | Country Code: +1
DXEngineering@DXEngineering.com

800-777-0703 | DXEngineering.com

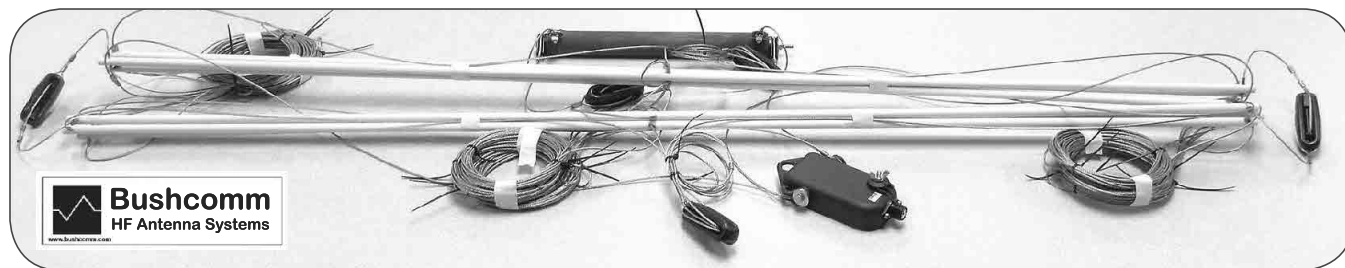
Exclusively at DX Engineering!



TransWorld Antenna Packages

The famed TransWorld Antenna is small and portable, yet offers exceptional performance and is durable enough even for a permanent installation.

DX Engineering has purchased TW Antennas to ensure the TransWorld Antenna will continue to be available. We've bundled them together in handy packages, search keyword "TransWorld" at DXEngineering.com to see them all.



Bushcomm HF Antenna Systems

Bushcomm is based in Australia, so its equipment is tested in the arid, wind-torn plains of the Outback. It is through these rigorous trials that Bushcomm has built its reputation for creating mission-critical antenna systems. Bushcomm gear is ideally suited for emergency and portable duty, but it performs well in mobile, base station, and marine applications too.

HF Multiplexers and Band-Pass Filters

Use Low Band Systems' Multiplexers to connect multiple radios to a single multi-band antenna, so you can use each radio to operate on a different band simultaneously. This reduces equipment installation hassles and saves money since there's no need for extra antennas and coax cable.

See the review in the March 2017 issue of QST.

The multiplexers work with Low Band Systems' multi-stage band-pass filters to limit the RF to a single band, effectively eliminating most RF interference issues. Sold separately, the filters deliver the isolation demanded by the multiplexer's band input.



KENWOOD ICOM YAESU ALINCO

See You at Hamvention®, Building One—Booths 1207-1210 and 1307-1311

Email Support 24/7/365 at DXEngineering@DXEngineering.com



Improve Performance of Your Octopus V/I Curve Tracer Using a Single Voltage Transformer

Perform in-circuit trouble shooting with this improved tester that provides selectable higher scanning voltages for testing.

Many hams enjoy experimenting with electronics and troubleshooting circuits. However, it is frustrating when we have no access to schematics or component identification, or when we need to remove the suspicious components from the board to check them individually. We might even finish by damaging the component or the board itself, or we might even get false readings with the multimeter, depending on the component. Fortunately, a simple and efficient way to overcome these problems has been around for decades. It consists in an electronic device connected to an oscilloscope. It has a number of designations, such as V/I (voltage/current) curve tracer, analog signature analyzer, component tester, oscilloscope test adapter, or simply “Octopus”. I constructed a basic Octopus after reading an article published by David Ludlow, W7QHX, in *QST*.¹ My device nicely accomplished the job with its single output of 1 V limited to 1 mA. As noted by David, the voltage and current are low enough for safe testing of almost any semiconductor circuit board assembly.

Recently I needed to check some unidentified Zener diodes and also a suspicious integrated circuit (IC) from my junk box, and required more optional voltages to trace possibly higher Zener voltages and IC junctions. After surveying the available literature, I found Octopus circuits using transformers with multi-tap voltages in the secondary. Because these transformers are hard to find, and re-winding

the secondary was out of question for me, I designed a simpler solution keeping my previous single-voltage secondary transformer by using multiple voltage dividers and current limiters. My Octopus had its range improved at an insignificant cost, and I got my junk box organized!

Octopus Basics

A curve tracer is a test equipment added to an oscilloscope — either digital or analog — that provides a graphical display of the V/I characteristic of an electronic component. It can be used to quickly check resistors, capacitors, inductors, semiconductors — both diodes and transistors — and, under some circumstances, integrated circuits.

The oscilloscope must have X-Y mode capability, which allows one channel to drive the horizontal amplifier (the X-channel), while the other (Y-channel) drives the vertical amplifier. The X-channel measures voltage, while the Y-channel measures current. This V/I testing permits an on-screen plot of I versus V. The device has a precise limited current applied to appropriate points on the device under test using common multimeter red and black leads. The measured voltage drop, current flow, and phase shift are plotted as the current versus voltage on the oscilloscope. The observed signatures, called Lissajous patterns, of known-good components or printed-circuit boards are compared with those of a suspect one. Unusual or unexpected signatures

indicate a potential problem. There are four fundamental components signatures: resistive, capacitive, inductive and semi-conductive. Recognizing and interpreting these four basic signatures is crucial to successful Octopus utilization.

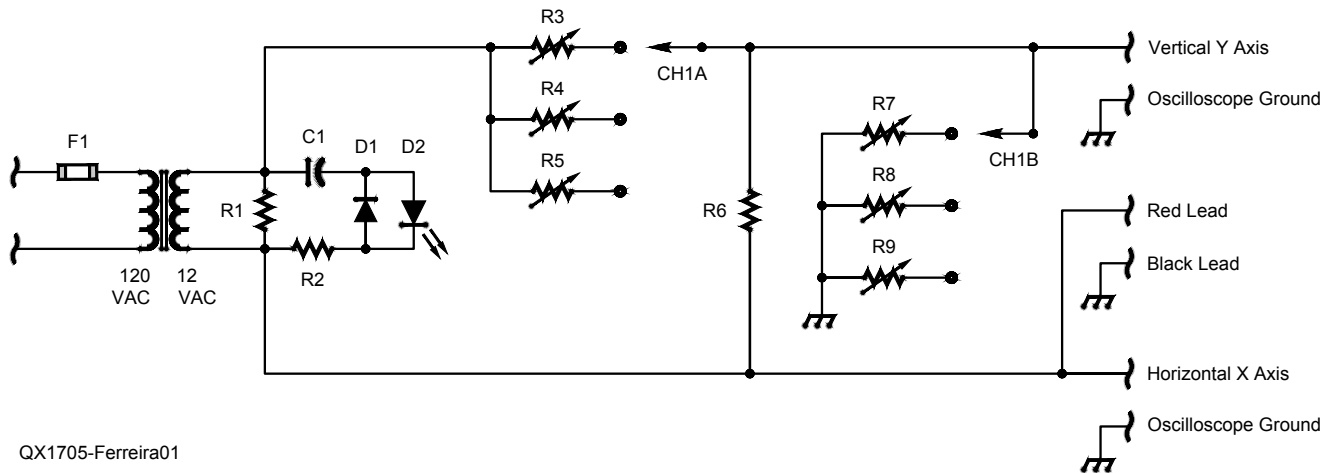
In-circuit tests are generally possible in many cases. However, complex Lissajous figures from resistors, capacitors and inductors connected to semiconductors can also be produced. In this case, we disconnect one terminal of the device under test (DUT) from the circuit. Once we are familiarized with Octopus operation, we can create a file of the measured Lissajous patterns of both normal isolated and in-circuit components for future comparisons.

Please keep in mind, the components, as well as the board itself must not be connected to the ac mains line or to a battery. No signal inputs are recommended. Remove all unnecessary cables from the equipment under test and disconnect any other line or electrical source.

A in-depth discussion of V/I testing and signature analysis is beyond the scope of this article, but very good overviews are available.^{2,3} Descriptions of oscilloscope X-Y modes may be found in ARRL publications.^{4,5}

Assembly and Settings

This Octopus V/I curve tracer supports three output voltages: 1 V ac, 5 V ac, and 10 V ac, each at about 1 mA. Figure 1 shows the circuit schematic diagram. Figure 2 shows



QX1705-Ferreira01

Figure 1 — Schematic diagram of the improved Octopus.

C1 — 470 nF, 400 V, ceramic capacitor
CH1 — Rotary switch, 2 poles, 3 positions
D1 — 1N4004 silicon diode or similar
D2 — Red LED
F1 — 1 A fuse and support
R1 — 1 k Ω ¼ W film resistor
R2 — 1 M Ω ¼ W film resistor

R3, R8, R9 — 10 k Ω variable resistor (trim pots)
R4, R5 — 2.2 k Ω variable resistors (trim pots)
R6 — 220 Ω ¼ W film resistor
R7 — 100 Ω variable resistor (trim pot)
R10 — 1 Ω ¼ W film resistor, or an approximate value

R11 — 50 Ω ¼ W film resistor, or an approximate value
T1 — 120 V ac primary, 12 V ac secondary, 500 mA transformer
 Various mechanical components, cables, and housing according to builder's preference.

a suggested PC board layout parts placement for the trimmer resistors, and Figure 3 shows a suggested component placement on the PC board that connects to the transformer and the ac mains. Neither of the PCB layouts nor the placement of components is especially critical. The components are commonly available and other component values may be substituted depending on your needs.

You will also need a multimeter with millivolts ac capability (or use the oscilloscope), a 20-30 W soldering iron, a drill for making the PC board holes, and various hand tools.

I started by assembling a rigid support for the 120 V ac input in a plastic box. I made a small circuit board, Figure 3, which was fixed to the bottom of the plastic housing using small screws and plastic separators. The board contains the connections to the LED red pilot, D2, and the wires of the transformer.

The switch CH1 must have at least 2 poles, A and B, and 3 positions (1 V, 5 V, 10 V) for a total of 6 taps connected to each of the 6 trimmer resistors. With your multimeter, identify and note which taps connect with the switch poles CH1A and CH1B in each one of the three positions. For practical purposes, I call CH1A the pole connected to voltage dividers (pole A) and CH1B, the pole connected to current limiters (pole B). Don't solder any wire to CH1 just yet.

Setting the voltage ranges

Solder the components on both PC boards and, then solder the 12 V ac wires into the Octopus board input. Don't connect any more wires at this time. Now, set the intended

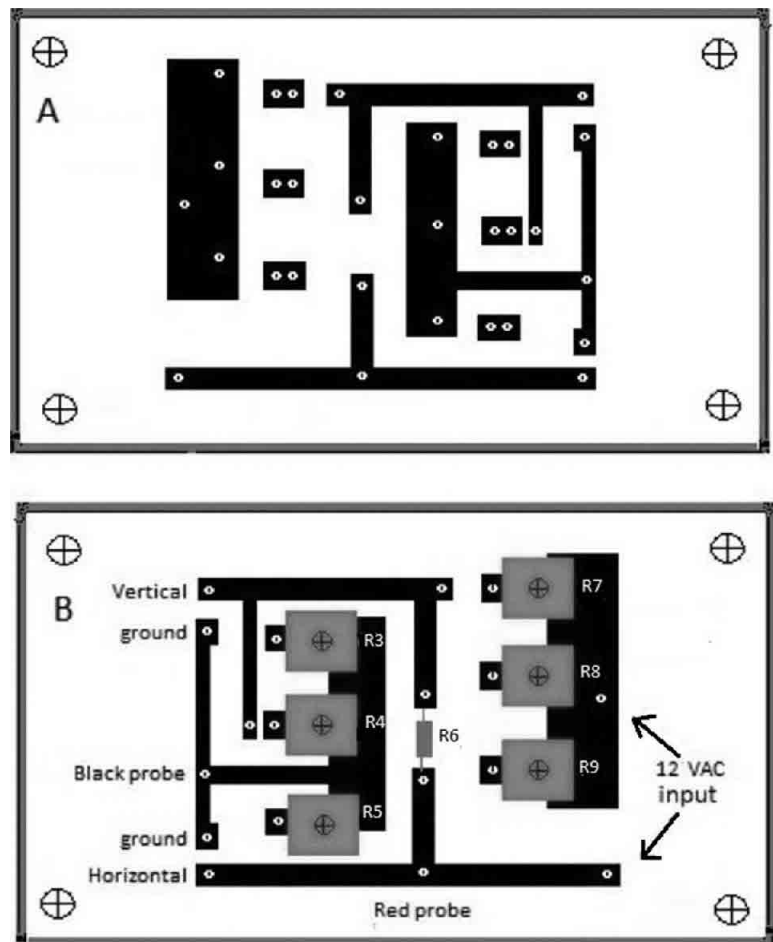


Figure 2 — Main PC board suggested layout.

output voltages following these steps.

(1) – Check to make sure that you have 12 V ac at the Octopus input. If so, solder a temporary jumper between CH1A and R3.

(2) – Set the variable resistor R3 for 1 V ac between the red and black lead outputs on the PC board. Then disconnect the temporary jumper from R3.

(3) – Connect the jumper from CH1A to R4. Set R4 for 5 V ac. Then disconnect the temporary jumper from R4.

(4) – Connect the jumper from CH1A to R5. Set R5 for 10 V ac. Then disconnect the jumper from R5 and keep it to CH1A.

Setting the current limits

Temporarily, make a sub-circuit shown in the dashed outline in Figure 4. On the PC board solder R10 to the red lead connection point and solder R11 in the black lead connection point. R11 will serve as a 50 Ω load for ac current readings. Set your multimeter to the millivolts ac scale, or use your oscilloscope for the measurement. Make sure the instrument is in parallel with R10. Since R10 is 1 Ω, then a voltage of 1 mV you read across R10 corresponds to a current of 1 mA.

(5) – Connect a jumper from CH1A to R3, and another jumper from CH1B to R7. Set R7 for approximately 1 mA (1 mV meter reading). When done, disconnect the jumpers from R3 and R7.

(6) – Connect the jumpers from CH1A to R4 and CH2B to R8. Set R8 for approximately 1 mA calculated through R10 (1 mV meter reading). Then disconnect the jumpers from R4 and R8.

(7) – Connect the jumpers from CH1A to R5 and CH2B to R9. Set R9 for approximately 1 mA calculated through R10 (1 mV meter reading). When done, disconnect these jumpers and the sub-circuit shown in dashed line of Figure 4.

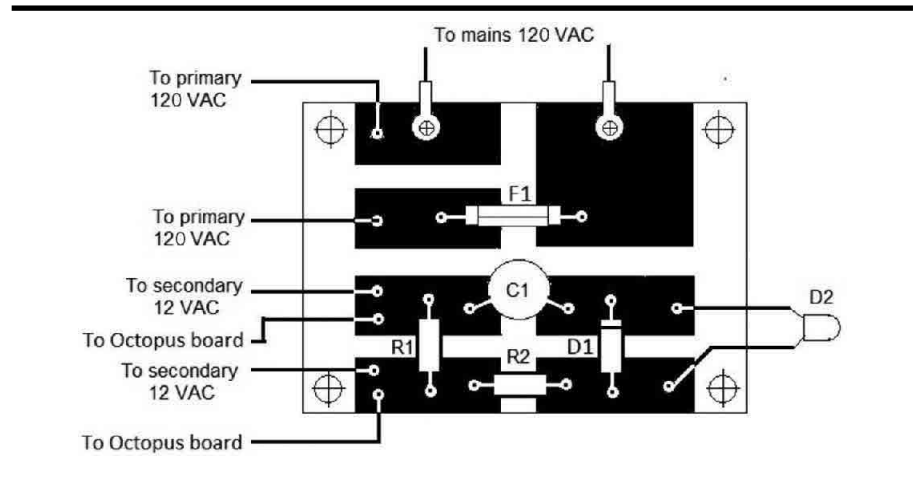
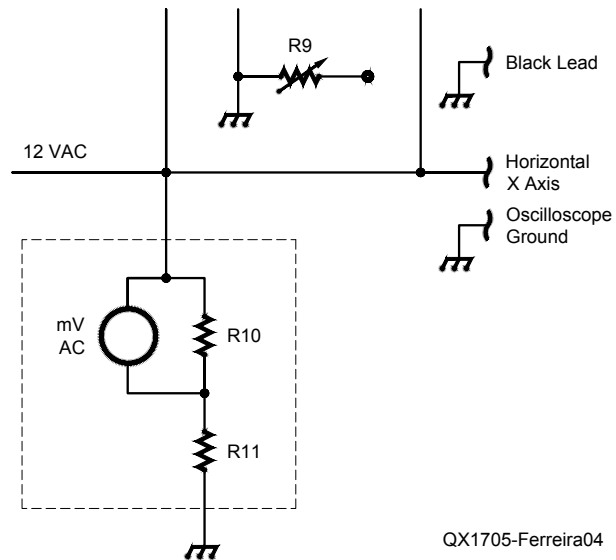


Figure 3 — Smaller PC board suggested layout.



QX1705-Ferreira04

Figure 4 — Temporary sub circuit designed for setting the Octopus output ac current limits.



Figure 5 — Internal view of the assembled Octopus.

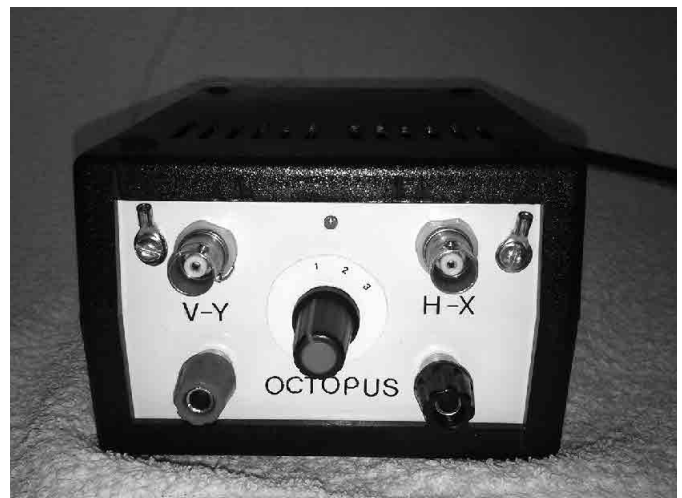


Figure 6 — Front view of the assembled Octopus.

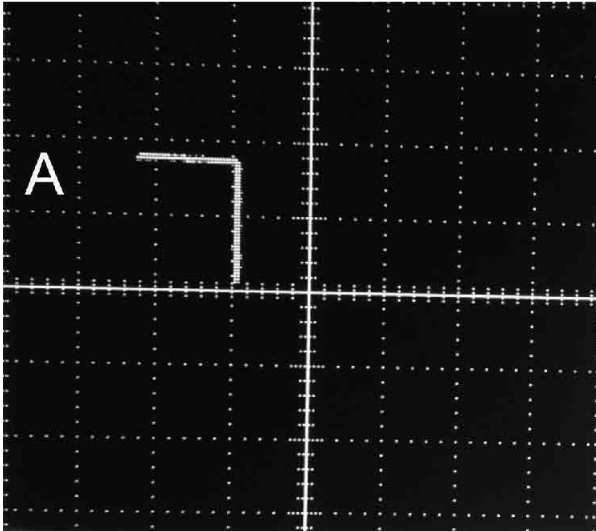


Figure 7A — I-V pattern for a 7V Zener diode with a 1 V sweep.

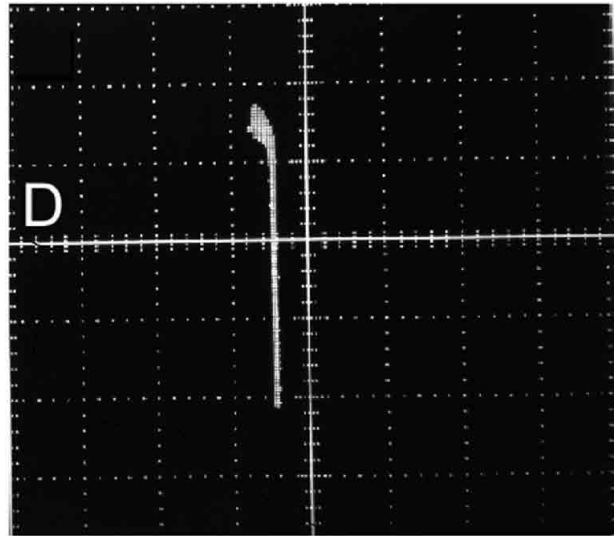


Figure 7D — I-V pattern for a healthy IC using a 1 V sweep.

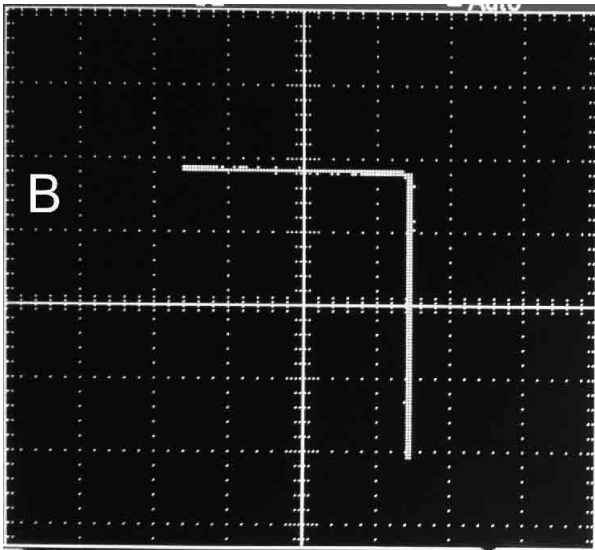


Figure 7B — I-V pattern for a 7V Zener diode with a 5 V sweep.

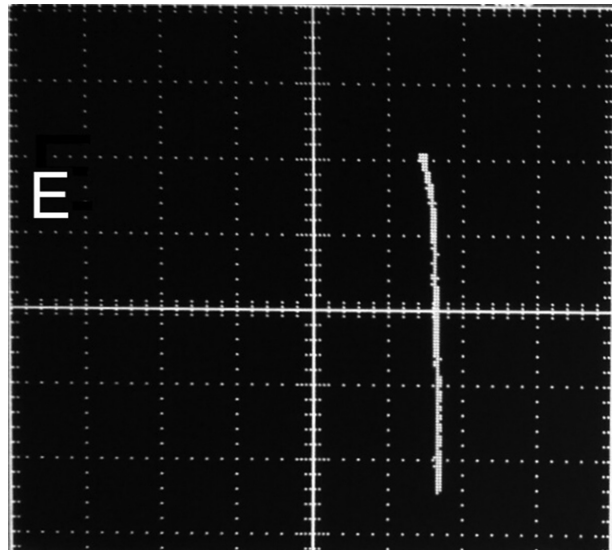


Figure 7E — I-V pattern for a damaged IC using a 1 V sweep.

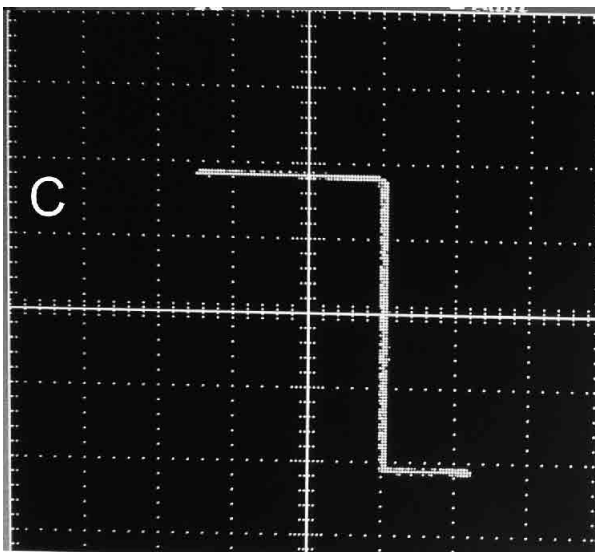


Figure 7C — I-V pattern for a 7V Zener diode with a 10 V sweep.

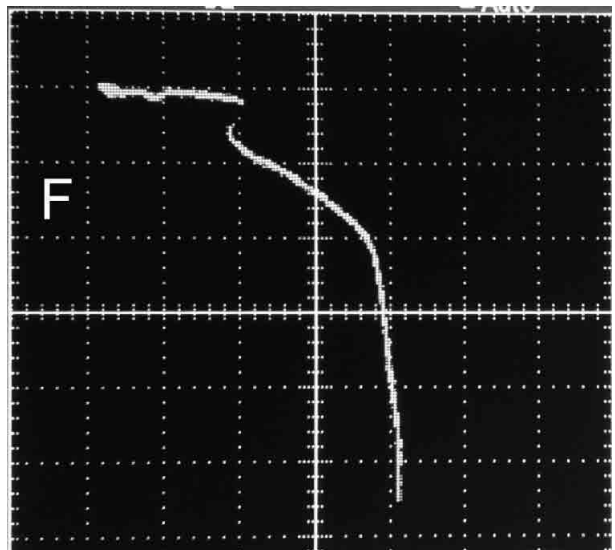


Figure 7F — I-V pattern for a damaged IC using a 5 V sweep reveals a distorted response.

Final Assembly

Once you have finished your PC board and set all the voltage and current limits, solder the connections from the CH1 poles to the respective sites on the PC board using different color wires. In position 1 (1 V selection), CH1A connects to R3 and CH1B, to R7. In position 2 (5 V selection), CH1A connects to R4 and CH1B to R8. In position 3 (10 V selection), CH1A connects to R5 and CH1B to R9. Install everything into the plastic housing, as seen in Figure 5.

Install the BNC connectors, and prepare two coaxial cables for connection to the oscilloscope. Figure 6 shows the front panel of the fully assembled Octopus.

Beyond 1 V

Set your oscilloscope to the X-Y mode and connect it to the Octopus. Set the Octopus to the 1 V position. Connect a 7 V Zener diode for testing. Try increasing the voltages from 1 to 5 and 10 V ac positions by rotating CH1 and observe how the I-V curves vary. Figure 7A shows the I-V response for the 7 V Zener diode with a 1 V sweep limited to 1 mA current. Figure 7B shows a sweep using 5 V ac limited to 1 mA, and Figure 7C shows a 10 V ac sweep with a 1 mA limit, which reveals the full performance of the diode. Clearly, the 7 V Zener diode cannot be properly evaluated using just the 1 V sweep.

A 1 V sweep of pin 5 referenced to ground

of a 555 IC is shown for a known good IC (Figure 7D) and a damaged IC (Figure 7E), but not much difference is evident. However, distortion is evident in Figure 7F on a 5 V sweep of the damaged IC

Now that you have your Octopus working, be sure to consider component voltage and current limitations before exposing components to different voltage values.

In Conclusion

The Octopus curve tracer is one of several ways available to test electronic components. The device described here is a simple alternative to get three different voltage ranges using a single secondary output transformer. Don't forget to disconnect the ac mains line or battery of the board under test, and don't overlook component voltage and current tolerances and limitations. With some practice, experience, and research you will be able to correctly interpret the measured Lissajous patterns.

Acknowledgment

I thank electronic engineer Rene Stelmach, formerly PY3CDW, for his comments and suggestions.

Paulo Renato F. Ferreira, PY3PR, is a radiation oncologist in Porto Alegre, RS, Brazil. He earned the MD and PhD degrees in Medicine. An ARRL member; he was first

licensed in 1979 at age 22 and now holds an Amateur A class license. Paulo has written technical contributions for QST, QSP (a Portuguese publication), Eletronica-Popular (a ceased Brazilian publication) and some web pages. His main radio interests are low-band DX, experimenting with homebrew antennas, analog electronics, CW rag-chewing and CW contests. He also enjoys bicycling and seashore fishing in Xangri-lá, RS, where he also has his Amateur Radio station.

Notes

¹D. Ludlow, W7QHX, "The Octopus", QST Jan 1975, pp 40-42.

²A. Lowne, "An analog signature analysis primer", www.electronicproducts.com/Test_and_Measurement/Benchtop_Rack_Mountable/An_analog_signature_analysis_primer.aspx.

³Huntron, Inc. "Fundamentals of Signature Analysis. An In-depth Overview of Power-off Testing Using Analog Signature Analysis", www.huntron.com/corporate/docs/ASA-paper-extract.pdf.

⁴The ARRL Handbook Book, 2017 Edition. ARRL item no. 0635 (hardcover) or 0628 (soft cover), available from your ARRL dealer, or from the ARRL Store, Telephone toll-free in the US 888-277-5289, or 860-594-0355, fax 860-594-0303; www.arrl.org/shop/; pubsales@arrl.org.

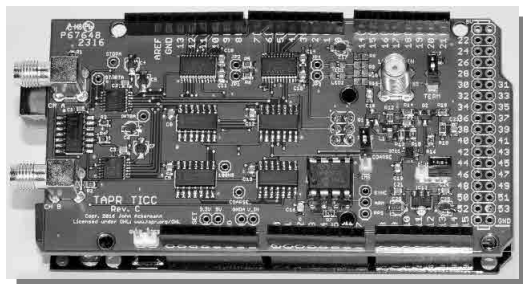
⁵Oscilloscopes for Radio Amateurs, Available from your ARRL dealer or the ARRL Bookstore, ARRL item no. 0976. Telephone 860-594-0355, or toll-free in the US 888-277-5289; www.arrl.org/shop/; pubsales@arrl.org.



20M-WSPR-Pi is a 20M TX Shield for the Raspberry Pi. Set up your own 20M WSPR beacon transmitter and monitor propagation from your station on the wspnet.org web site. The TAPR 20M-WSPR-Pi turns virtually any Raspberry Pi computer board into a 20M QRP beacon transmitter. Compatible with versions 1, 2, 3 and even the Raspberry Pi Zero!

TAPR is a non-profit amateur radio organization that develops new communications technology, provides useful/affordable hardware, and promotes the advancement of the amateur art through publications, meetings, and standards. Membership includes an e-subscription to the *TAPR Packet Status Register* quarterly newsletter, which provides up-to-date news and user/technical information. Annual membership costs \$25 worldwide. Visit www.tapr.org for more information.

NEW!



TICC

High-resolution 2-channel Counter

The **TICC** is a two channel counter that can time events with 60 **picosecond** resolution. It works with an Arduino Mega 2560 processor board and open source software. Think of the most precise stopwatch you've ever seen, and you can imagine how the TICC might be used. The TICC will be available from TAPR in early 2017 as an assembled and tested board with Arduino processor board and software included.



TAPR

PO BOX 852754 • Richardson, Texas • 75085-2754

Office: (972) 671-8277 • e-mail: taproffice@tapr.org

Internet: www.tapr.org • Non-Profit Research and Development Corporation

Octave for Complex Characteristic Impedance

If you are interested in precise calculations, you might want to think about what the low and high frequency approximations to transmission lines actually mean.

Most of us are used to seeing the characteristic impedances of various transmission lines listed as 75 Ω, 52 Ω, 600 Ω, and so on. How about (416.95 - j403.06) Ω? We're used to seeing network impedances or impedances along a transmission line specified as complex, but not transmission line characteristic impedances. Why not? Usually, we hams are working at frequencies high enough so that the high frequency approximations apply. Let's review how we get to those approximations.

The Approximations

The exact expression for the characteristic impedance of a line¹ is:

$$Z_0 = \sqrt{\frac{R + j\omega L}{G + j\omega C}} \quad (1)$$

where

Z_0 = characteristic impedance of the transmission line

R = distributed series resistance in ohms per unit length

L = distributed series inductance in henry per unit length

G = distributed shunt conductance in siemens per unit length

C = distributed shunt capacitance in farad per unit length

ω = radian frequency is $2\pi f$ hertz.

High Frequencies

When the frequency is high, above a few hundred kilohertz, $j\omega L$ is usually much higher than R , and $j\omega C$ is much higher than G . so R and G can then be neglected and Equation (1) reduces to²,

$$Z_0 = \sqrt{\frac{L}{C}} \quad (2)$$

Because L and C in this approximation are always real, Z_0 is also always real or very close to real, at high frequencies and is relatively constant (independent of frequency) over a broad range of frequencies.

Low Frequencies

At relatively low frequencies, say 1 kHz, the decrease in ω causes R to predominate in the numerator and $j\omega L$ may be neglected. In the denominator however, G decreases very rapidly as the frequency is lowered and $j\omega C$ remains predominant in the denominator. A low frequency approximation valid for many lines³ is then,

$$Z_0 = \sqrt{\frac{R}{j\omega C}} \quad (3)$$

The phase angle of $R/j\omega C$ is -90 degrees, which after the square root operation is -45 degrees. The value "416.95 - j403.06" mentioned above is the characteristic impedance at 1 kHz of a typical #22 AWG pulp-insulated telephone cable twisted pair, calculated using all four primary constants.⁴ In polar coordinates (416.95 - j403.06) Ω = (579.92 Ω at -44.030°). Note that the phase angle here is very close to that of our low frequency approximation.

Precise Calculation

For the most part hams need not care about this. Most of our transmission lines are operated at frequencies at which the high frequency approximations are sufficiently

accurate for most practical purposes. If, however, we are interested in precise calculations, we might want to think about what the high frequency approximation to Z_0 actually means. Going back to the exact expression Equation (1) for Z_0 , we can make the expression real by establishing the relationship,

$$\frac{R}{L} = \frac{G}{C} \quad (4)$$

This is known as the Heaviside Condition for a Distortionless Line.⁵ Note that distortionless doesn't mean lossless. Although series inductive loading is used in voice frequency telephone cable pairs to bring Z_0 closer to the Heaviside condition⁶, practical high frequency transmission lines never approach this condition. The only other way to make Z_0 real at high frequencies is to set R and G to zero. That means a line with no attenuation as we are removing all the impairments that can absorb energy as a wave travels along the line. Z_0 for such a line is well approximated by Equation (2).

All of our practical transmission lines attenuate signals by absorbing energy in the series resistance, R , of the conductors and in the parallel conductance, G , of the dielectric between the conductors. So we approximate Z_0 in a manner that requires that there is no attenuation, and we then calculate attenuation and phase shift (the propagation constant) using approximations that conflict with those used for Z_0 . Because the attenuation of our high frequency lines is usually low in decibels per wavelength⁷, we can usually tolerate these "mismatched" approximations.

As we move lower in frequency, to MF frequencies lower than 160 meters and to the LF band, or if we need to work with voice frequency lines of appreciable length, the high frequency approximations may not serve us well. A manifestation of even a small imaginary component of characteristic impedance is an error in the calculation of reflection coefficient and *VSWR*. Chipman points out (see Note 7) that the concept of *VSWR* is "... valid only on lines which have low attenuation per wavelength, since it is only for this case that the concept of voltage standing-wave ratio has a useful empirical meaning."

We can explore a limiting case by assuming a characteristic impedance with a phase angle of -45 degrees and then terminating it in a conjugate impedance with a phase angle of +45 degrees. The reflection coefficient, ρ , is given by⁸ as

$$\rho = \frac{Z_t - Z_0}{Z_t + Z_0} \quad (5)$$

where Z_t is the impedance terminating the transmission line.

Since the real and reactive components are equal in magnitude for a phase angle of 45 degrees, we'll let $N = R_0 = |X_0|$. The reflection coefficient for such an interface would be, for any real valued N ,

$$\rho = \frac{(N + jN) - (N - jN)}{(N + jN) + (N - jN)} = j$$

VSWR is given⁹ by:

$$VSWR = \frac{1 + |\rho|}{1 - |\rho|} \quad (6)$$

Plugging our value for ρ in here, we get

$$VSWR = \frac{1 + |j|}{1 - |j|} = \infty$$

meaning that a conjugate match that actually provides the maximum power transfer across the interface yields a very bad error in the calculation of *VSWR* in that it predicts reflection of all the power, and transmission of none.

This extreme example, which is not very much unlike the actual case for voice frequency lines that we discussed earlier, illustrates why telephone engineers generally use reflection loss and return loss calculations, rather than reflection coefficient and *VSWR* for cable pair calculations. Although *VSWR* is described along with return loss and reflection loss in Note 9, we point out that the concept of *VSWR* depends on a near zero attenuation of the line. Even for frequencies well within the range for which the high frequency approximations are

valid, comparisons of calculations of line loss using τ equivalent networks¹⁰ and reflection loss and *VSWR* expressions will show some variance unless the characteristic impedance used in the calculations is real. Steve Stearns, K6OIK, points out that "ignoring the seemingly small imaginary part of Z_0 of practical transmission lines can give large errors in predicted delivered power".¹¹

This issue was surfaced¹² by Larry Bos, W0PSI, when he was working with relatively precise calculations of secondary constants for transmission lines at high frequencies and noticed that, when he didn't neglect the imaginary part of the characteristic impedance, the line loss predicted by the τ equivalent network of *Octave for SWR*¹³ disagreed with that predicted by the *VSWR* calculations in the *ARRL Handbook*.¹⁴ Larry made a number of useful calculations, which illustrate that in some cases, the errors introduced to *VSWR* calculations by the imaginary component of Z_0 may be significant for HF applications or may cause errors in the results of calculations that might cause us to suspect that our math is faulty even if the errors themselves are small.

ABCD Matrix Octave Code

Just for verification of our earlier *GNU Octave* code¹⁵, and to introduce a different transmission line modeling technique, we will add to our *GNU Octave* code for transmission lines an *ABCD* matrix simulation of a transmission line.¹⁶ The *ABCD* matrix, sometimes called a transmission matrix¹⁷, can be used to simulate a transmission line or a network of discrete elements. The elements of the matrix represent complex ratios that are indicative of transmission in both directions through the simulated network and of the input impedance of each port. An *ABCD* matrix representing a transmission line in terms of its secondary constants is,

$$\begin{vmatrix} V_{IN} \\ I_{IN} \end{vmatrix} = \begin{vmatrix} A & B \\ C & D \end{vmatrix} \begin{vmatrix} V_{OUT} \\ I_{OUT} \end{vmatrix} \quad (7)$$

where:

$$A = \cosh(\gamma d)$$

$$B = Z_0 \sinh(\gamma d)$$

$$C = Z_0 \sinh(\gamma d) / Z_0$$

$$D = \cosh(\gamma d)$$

α = attenuation of line per unit length

β = phase shift of line in radians per unit length

$$\gamma = \alpha + j\beta$$

d = length of line

A , B , C , D and γ are defined above according to the literature (see Notes 16 and 17). In the code listed in Table 1, γ has been

multiplied by d to produce a new variable, γ_{total} , which is used in the definitions of A , B , C , and D to avoid four multiplications by d .

The *ABCD* matrix transforms the column matrix representing the output voltages and currents of the transmission line into a column matrix representing the input voltage and current. Solving the matrix for the input currents and voltages we have,

$$V_i = AV_i + BI_i \quad (8)$$

$$I_i = CV_i + DI_i \quad (9)$$

Although I prefer the τ equivalent network for most transmission line simulations, the *ABCD* matrix is convenient when multiple independent transmission line sections are connected in tandem and/or with other networks that can be described in matrix format. *GNU Octave* features some powerful matrix tools that make handling matrices easy and efficient. We haven't used them much in this series and, in fact, we stayed with the τ equivalent network in *More Octave for Transmission Lines* (see Note 10) when we connected lines in tandem as we were already working with that network. The τ equivalent network, in my opinion, provides a more intuitive transmission line model than does the *ABCD* matrix although others may disagree.

Here, we will implement the *ABCD* matrix to independently verify the τ equivalent network code we were already using in this series while incidentally adding another tool to our *Octave* toolbox.

We'll do this by reusing code from *More Transmission Lines for Octave* (see Note 10) and *Octave for SWR* (see Note 13) and adding new *Octave* code to implement the equations derived from the *ABCD* matrix. The resulting code is listed in Table 1. Although we have often, for brevity, let the text in the article comment the code in this series, here the code is lengthy and segmented enough so that it will be of advantage to embed a few comments in the code. The output of a run with the secondary constants that are included in the code in Table 1 is listed in Table 2. Note that the τ equivalent network and the *ABCD* matrix methods produce the same output, but the equation for *VSWR* from the *ARRL Handbook* (Note 14) differs a bit from those two when Z_0 is complex, even when the imaginary component is small compared to the real component of Z_0 .

Why do we see this problem with reflection coefficient and *VSWR*? A clue would be the use of the absolute value of ρ in calculating *VSWR*, a step which discards the phase information contained in ρ . When the attenuation is not zero, and both the incident and reflected waves vary in amplitude

along the line, the phase information at the reflection point is vital in understanding how the two waves combine with each other to produce standing waves. There is, in fact, no literally accurate value of *VSWR* at any point along the line with attenuation because the maximum amplitude, where the two waves exhibit maximum reinforcement, and the adjacent minimum amplitude, where the two waves exhibit maximum partial cancellation, are at points where the *VSWR*, if it were possible to calculate it accurately, would be different. Chipman comments¹⁸: “Since all maxima and minima in any standing wave pattern occur at different values of *d* (distance along line from load), it appears from this equation that in a pattern on a line with attenuation all the maxima and minima will each have different magnitudes. This suggests that the *VSWR* concept and its uses may not be applicable.”

Texts on transmission lines generally handle the mathematics involved with these matters correctly, but the information is often somewhat buried. Chipman, for instance, states several pages into his chapter “Impedance Relations”, (see Note 8) that “In the remainder of this section, and in Sections 7.3, 7.4, and 7.5, all stated relations between the voltage reflection coefficient, ρ_r , and the normalized terminal load impedance Z_T/Z_0 are true when Z_0 is real but many of them are not true if Z_0 is complex”. Paris and Hurd¹⁹ state that “The exact solution of the boundary-value problem for lossy transmission lines is very involved, and in most cases cannot be obtained in closed analytical form”. They go on to describe an approximate method, a perturbation approach, that is often used to handle lossy lines. Note that Chipman writes in terms of complex Z_0 and Paris and Hurd in terms of lossy lines, but the two conditions are mathematically equivalent as we noted above. Chipman gives some rules of thumb for using adjacent maxima and minima to determine the *VSWR*. He states that the inequalities $\alpha/\beta \ll 1$ and $|\rho| < 0.5$ should allow the determination of the *VSWR* with useful accuracy (see Note 17).

Chipman also provides an expression (his Equation 8.15) for calculating the voltage along the transmission line as a function of the distance from the load.²⁰ Since Chipman is not interested in absolute, but only relative voltages here, and since he is writing before the advent of easy access to computers, he simplifies by omitting a scale factor term and the resulting equation (his Equation 8.17) is,

$$|V(d)| = \sqrt{\sinh^2 p + \cos^2(\beta d + q)} \quad (10)$$

where

Table 1

Octave code, see also www.arrl.org/qexfiles.

```
f = 7.01; # FREQUENCY IN MHZ
d = 100; # LENGTH OF LINE IN FEET
a = 2.0; # ATTENUATION IN dB PER 100 FEET
v = 66; # VELOCITY FACTOR AS A PERCENTAGE
#Zo = 50;
Zo = 50 - 1j * 0.72; # CHARACTERISTIC IMPEDANCE IN OHMS
# Specify source (transmitter) and load (antenna)
VS = 2.0;
RS = 50;
Rt = 100;
Xt = 0;
# Convert inputs as required
a = a ./ 1e2; # convert dB per 100 feet to dB per foot
a = 0.1151 .* a; # convert dB to nepers
c = 9.836e8; # speed of light in feet per second
lambda = c ./ (1e6 .* f); # wavelength of signal in vacuum
lambda = (v ./ 1e2) .* lambda; # adjust lambda for velocity
B = (2 .* pi) ./ lambda; # calculate Beta
ZL = Rt .+ j .* Xt; # calculate complex terminating impedance
# Calculate elements of T-equivalent network
# ZA = input series element
# ZB = output series element
# ZC = shunt element
ZA = Zo .* tanh((a .+ j .* B) .* d ./ 2.);
ZB = ZA;
ZC = Zo ./ sinh((a .+ j .* B) .* d);
# Prepare matrices for solution of currents
right_side = [RS + ZA + ZC, -ZC; -ZC, ZB + ZC + ZL];
left_side = [VS; 0];
# Solve for currents
denom = det(right_side);
for m = 1: rows(right_side)
    numerator = right_side;
    for n = 1: rows(right_side)
        numerator(n, m) = left_side(n);
    endfor
    current(m) = det(numerator) / denom;
endfor
# Calculate T-network input impedance
Zd = ZA .+ (ZC .* (ZB + ZL)) ./ (ZC .+ ZB .+ ZL);
# Calculate input power to T-network from source
Pwr_in = abs(current(1)) ^ 2 * real(Zd);
# Calculate power delivered by T-network to load
Pwr_load = abs(current(rows(right_side))) ^ 2 * real(ZL);
# Calculate T-network line loss
Line_loss = 10 * log10(Pwr_in / Pwr_load);
printf("\n T-NETWORK LINE LOSS (in dB) = %-8.5g", Line_loss);
# Calculate coefficients of ABCD matrix and solve
# for input voltage and current
Vt = 1.0;
gamma_l = (a + 1j * B) * d;
A = cosh(gamma_l);
B = Zo * sinh(gamma_l);
C = sinh(gamma_l) / Zo;
D = cosh(gamma_l);
It = Vt / ZL;
Vi = A * Vt + B * It;
Ii = C * Vt + D * It;
# Calculate ABCD matrix input impedance
Zin = Vi / Ii;
# Calculate input power to line (ABCD matrix) from source
Pwr_in = abs(Ii ^ 2) * real(Zin);
# Calculate power dissipated in load
Pwr_out = abs(It ^ 2) * real(ZL);
# Calculate and print out ABCD matrix line loss
Line_loss = 10 * log10(Pwr_in / Pwr_out);
printf("\n ABCD MATRIX LINE LOSS (in dB) = %-8.5g\n", Line_loss);
# Calculate and print out ARRL Antenna Book Total Loss (Eq. 16)
refl_coef = (ZL - Zo) / (ZL + Zo);
SWR = (1 + abs(refl_coef)) / (1 - abs(refl_coef));
adB = a / 0.1151;
mlr = 10 ^ (d * adB / 10);
Total_loss = 10 * log10((mlr ^ 2 - abs(refl_coef) ^ 2) / ...
(mlr * (1 - abs(refl_coef) ^ 2)));
printf(" ARRL EQ. 16 TOTAL LOSS (in dB) = %-8.5g\n\n", Total_loss);
```

$$p = -\ln(\sqrt{|\rho|}), \quad q = -\frac{\phi}{2}, \text{ and}$$

ϕ = angle of the reflection coefficient, and the omitted scale factor is,

$$\text{scale_factor} = \left| 2V_1 \exp(-\gamma l) \sqrt{\rho} \right|. \quad (11)$$

Chipman also provides expressions for

upper and lower asymptotes to the train of maximum and minimum voltages along the line.²¹ Since we're using a computer here, we'll use his Equation 8.15 instead, which he states is completely general. In Table 3, we've implemented Equation 8.17 and then multiplied by the omitted scale factor, which gets us to Equation 8.15, so that we can

display accurate voltages on the ordinates of Figures 1 and 2.

The only change we'll make is to change γ in the scale factor to $-j \text{Im}\{\gamma\}$ in the *Octave* code since the original scale factor in Equation 8.15 provides accurate results only when α is zero (a lossless line). Note that γ is a complex number but $\text{Im}\{\gamma\}$ is returned by *Octave* as a real value so we need to supply the imaginary operator in our code. The resulting scale factor we'll use, in *Octave* code, is

$$\left| 2V_1 \exp(-j\beta l) \sqrt{\rho} \right| \quad (12)$$

Since we're trying to accurately represent the voltages along the line in our plots, are the increasing levels of each asymptote and the enclosed standing wave toward the transmitter (to the right) accurate? We'll go to the right end of our plot and measure the values of the upper and lower asymptotes by asking the script for `upper_bound(1)` and `lower_bound(1)`. We can do this by simply entering the names of the elements on separate lines in the code, at any point in the code after the array holding the two variables has been defined, with no semicolon at the end of each line. We get about 1.9555 V for the upper and 1.3506 V for the lower asymptotes. Since the asymptotes represent the sums and differences of the incident and reflected waves along the line, we can solve for V_1 and/or V_2 using two equations in two unknowns:

$$\text{Upper asymptote} = V_1 + V_2$$

$$\text{Lower asymptote} = V_1 - V_2$$

Adding the two gives:

$$\text{Upper asymptote} + \text{Lower asymptote} = 2 * V_1$$

$$V_1 = 1.6531 \text{ volts.}$$

Since we specified V_1 as 1.0 V at the load,

Table 2

Octave code, see also www.arrl.org/qexfiles.

Zo = 50 ohms:

T-NETWORK LINE LOSS (in dB) = 2.3145

ABCD MATRIX LINE LOSS (in dB) = 2.3145

ARRL EQ. 16 TOTAL LOSS (in dB) = 2.315

Zo = 50 - j0.72 ohms:

T-NETWORK LINE LOSS (in dB) = 2.2907

ABCD MATRIX LINE LOSS (in dB) = 2.2907

ARRL EQ. 16 TOTAL LOSS (in dB) = 2.3151

Table 3

Octave code, see also www.arrl.org/qexfiles.

graphics_toolkit gnuplot;

#gamma = 1j * 0.5; # Used to generate Figure 1

gamma = 0.01 + 1j * 0.5; # Used to generate Figure 2

V1 = 1.0;

V2 = 0.5;

rho = V2 / V1;

p = log(1 / sqrt(abs(rho)));

q = -0.5 * arg(rho);

l = 16 * pi;

z = linspace(0, l, 200);

d = l .- z;

Vdabs = sqrt((sinh(real(gamma) .* d .+ p)) .^ 2 + (cos(imag(gamma) .* d .+ q)) .^ 2);

scale_factor = abs(2 .* V1 * e .^ (-1j .* imag(gamma) .* l) .* sqrt(rho));

Vdabs = scale_factor .* Vdabs;

upper_bound = scale_factor .* cosh(real(gamma) .* d .+ p);

lower_bound = scale_factor .* sinh(real(gamma) .* d .+ p);

plot(d, Vdabs, d, upper_bound, d, lower_bound);

grid();

xlabel("DISTANCE ALONG LINE => TOWARD TRANSMITTER");

ylabel("LINE VOLTAGE: ABSOLUTE VALUE");

pause;

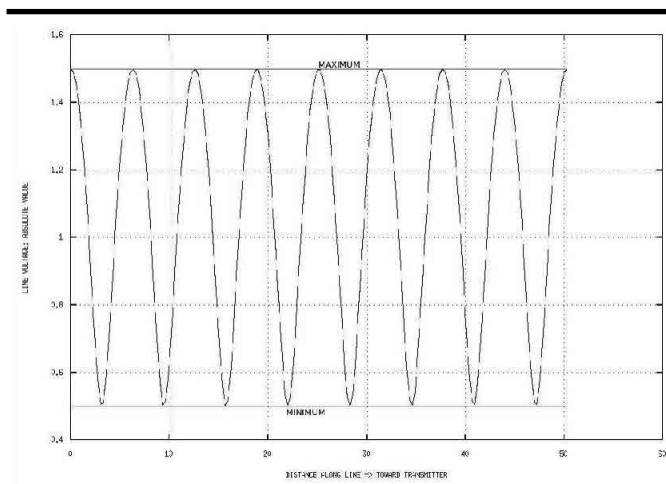


Figure 1 — Voltage along a transmission line with no attenuation.

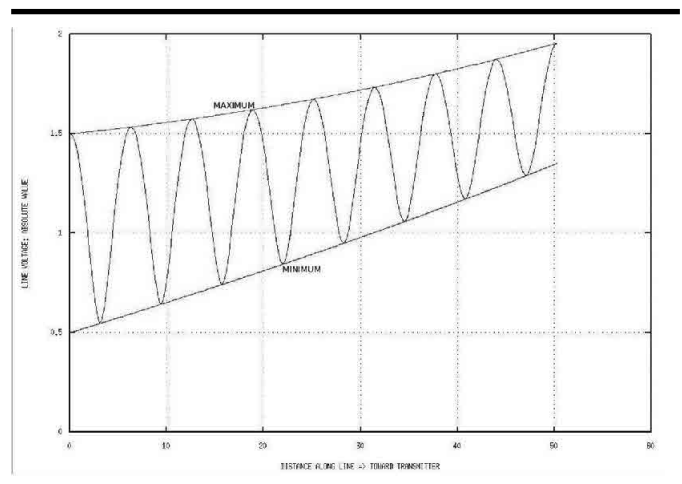


Figure 2 — Voltage along a transmission line with attenuation.

the loss from the transmitter to the load is $\ln(1.6531) = 0.5027$ Np. That loss occurs over 50 unit lengths of line, so the loss per unit length is $0.5027/50 = 0.01005$ Np per unit length, the same, within round-off error, as the loss per unit length we specified as the real part of γ in Table 3. This verifies that our plot represents the proper decay of the waveform along the line when we add attenuation. Once we've done this, it becomes obvious that the voltage we are seeking is the average of the upper and lower bounds, making it simpler to find in the future.

So we have a routine that will plot for us the combined forward and reflected voltages and *VSWR* envelope at any point along the line whether Z_0 is real or complex. We can also handle any complex reflection coefficient and resulting *VSWR* because voltages V_1 and/or V_2 , the forward and reflected voltages at the junction of the line and the load, may be specified as real, imaginary, or complex.

We'll use the *Octave* code in Table 3 to plot these curves for a line with no attenuation (Figure 1) and a line with substantial overall attenuation but with low attenuation per wavelength (Figure 2). The load — usually an antenna — is at the left end of each figure and the distance in radians proceeds toward the transmitter to the right. In our case, one radian is also one unit length. From Figure 1, where the attenuation is zero, we see that all the maxima have the same amplitude and all the minima have the same amplitude. We can calculate the *VSWR* accurately as the ratio between any maximum and any minimum.

In Figure 2, where the attenuation is non-zero, adjacent maxima and minima represent different vertical distances — differences in absolute voltage — between the asymptotic curves. There is no one pair at any location that represents a single *VSWR*, although the differences in this example are not great. As noted above, Chipman's opinion is that this may invalidate the use of *VSWR* as an indicator for lines with attenuation. Chipman may, though, have been thinking of *VSWR* measurements along a physical transmission line where voltage measurements are made at adjacent maxima and minima. Where we are calculating *VSWR*, rather than measuring it, the difference between the upper and lower asymptotes at any one point along the line will be sufficient to determine the *VSWR* at that point.

Summing Up

So what does all this mean? We've added two useful tools to our *GNU Octave* toolbox: a new modeling technique, the *ABCD* matrix, and a method for graphing the voltage maxima and minima along any line whether Z_0 is real or complex. We may conclude from this that:

(1) — Any line with attenuation must also exhibit a complex characteristic impedance.

(2) — In most HF applications, the difference between approximate and exact methods of determining line loss will be negligible but may be noticeable during precise calculations.

(3) — In voice frequencies (VF) applications, and in some MF and LF applications, the length of line and the magnitude of the imaginary part of the characteristic impedance will determine whether or not the complex impedance matters.

(4) — We can use the *ABCD* matrix for modeling transmission lines where there are advantages to that method over the T-equivalent network.

(5) — We can use the script in Table 3 to plot the voltage as a function of distance along a transmission line, along with curves asymptotic to the maximum and minimum values of voltage.

(6) — By making changes described by Chipman²², we can, if required, plot current maxima and minima instead of voltage maxima and minima.

Acknowledgement

My thanks go to Larry Bos, WØPSI, for the idea for this article and for his very helpful comments, suggestions and corrections.

Maynard Wright, W6PAP, was first licensed in 1957 as WN6PAP. He holds an FCC General Radiotelephone Operator License with Ship Radar Endorsement, and is a Registered Professional Electrical Engineer in California. He is a Life Senior Member of IEEE. Maynard was involved in the telecommunications industry for over 48 years, and has served as technical editor of several telecommunications standards, and holds several patents. He is a past Chairman of the Sacramento Section of IEEE. Maynard is past Secretary/Treasurer and Past President of the North Hills Radio Club in Sacramento, California.

Notes

¹Reference Data for Radio Engineers, Fourth Edition, International Telephone and Telegraph Corporation, 1956, p 552.

²Page 20.3 in, *The ARRL Handbook Book*, 2017 Edition. ARRL item no. 0628, available from your ARRL dealer, or from the ARRL Store, Telephone toll-free in the US 888-277-5289, or 860-594-0355, fax 860-594-0303; www.arrl.org/shop/; pubsales@arrl.org.

³G. S. Eager, Jr., J. Jachimowicz, I. Kolodny, D. E. Robinson, AIEE Paper 59-778, "Transmission Properties of Polyethylene Insulated Telephone Cables at Voice and Carrier Frequencies", *The American Institute of Electrical Engineers*, 1959, p 6.

⁴Primary constants calculated from polynomial approximations listed in Table 8-6 on p 559 of Roger L. Freeman, *Reference Manual for Telecommunications Engineering, Second Edition*, John Wiley & Sons, 1994.

⁵R. A. Chipman, *Schaum's Outline Series - Theory and Problems of Transmission Lines*, McGraw-Hill, 1968, p 49.

⁶B. Whitfield Griffith, Jr., *Radio-Electronic Transmission Fundamentals*, McGraw-Hill, 1962, pages 197-198.

⁷Chipman [Note 5], p 190.

⁸Chipman [Note 5], p 128.

⁹*Telecommunications Transmission Engineering, Volume 1, Principles*, Bell System Center for Technical Education, 1974, pp 126-130, 133-134.

¹⁰M. Wright, W6PAP, "More Octave for Transmission Lines", *QEX*, Jan/Feb, 2008.

¹¹Steve Stearns, K6OIK, "A Transmission Line Power Paradox and Its Resolution", *ARRL Pacificon Antenna Seminar*, Santa Clara, CA, 2014, p 50.

¹²Personal correspondence between Larry Bos, WØPSI, and Maynard Wright, W6PAP.

¹³M. Wright, W6PAP, "Octave for SWR", *QEX*, Jan/Feb, 2009.

¹⁴*The ARRL Handbook for Radio Communications, 2015*, The American Radio Relay League, Inc., 2014, page 20.4.

¹⁵GNU Octave, www.octave.org.

¹⁶Reference Data for Radio Engineers, p 660.

¹⁷Chipman [Note 5], p 142.

¹⁸Chipman [Note 5], p 167.

¹⁹D. T. Paris and F. Kenneth Hurd, *Basic Electromagnetic Theory*, McGraw-Hill, 1969, p 399.

²⁰Chipman [Note 5], p 164.

²¹Chipman [Note 5], Figure 8-9, page 168.

The code expression for the lower asymptote is: $\sinh(\alpha \cdot d+p)$ and for the upper asymptote is: $\cosh(\alpha \cdot d+p)$.

²²Chipman [Note 5], p 178.

Polarization in HF Atmospheric Noise

Measurements show that vertically and horizontally polarized noise can differ by tens of decibels in the lower HF bands.

I was struggling to design an HF system for an international customer located in the tropics. The customer wanted to communicate between two specific points, but no matter what I did, I could not *reasonably* deliver a sufficient receiver signal to noise ratio (SNR). I looked harder at the atmospheric noise per the ITU predictions [ITU-R-372-9 and CCIR-322 noise data measurements used a standard ground-mounted vertically polarized monopole.—*Ed.*].¹ Results looked unsatisfactory. In my teenage days, as a fledgling ham, I was taught by a mentor that vertical antennas on vehicles always suffered higher levels of ignition noise than horizontal ones. I wondered if atmospheric noise varied with polarization. An Internet search yielded a 1968 study by George Hagn and his colleagues detailing a rigorously-conducted comparative measurement of atmospheric noise versus frequency, polarization, direction of arrival, and time-of-day.²

A Historical Note

I started my radio engineering career at Collins Radio in 1969, and saw a wide span of HF communication systems and techniques developed during the 1960s. This was before the satellite communications era; HF was the only long-haul communications medium between southeast Asia and the continental US. Military communication planners had reached the same impasse that I reached in trying to make the HF communication circuits work. They too wondered if a horizontal or a vertical antenna offered any performance advantage in that environment.

Table 1

Horizontally polarized antenna noise advantage. Source: Hagn [Note 2] Figure 16, “Comparison of ARN-2 Monopole and trapped dipoles observed noise, with CCIR Report 322 Predictions, Thailand, Autumn 1967”.

Local time, hours	2.3 MHz	5 MHz	10 MHz
00-04	19 dB	9 dB	3 dB
05-08	25 dB	8 dB	5 dB
09-12	32 dB	18 dB	3 dB
13-16	30 dB	20 dB	1 dB
17-20	26 dB	10 dB	4 dB
21-00	21 dB	10 dB	3 dB

Abstract from Special Technical Report 47

HF Atmospheric Radio Noise on Horizontal Dipole Antennas in Thailand

“The noise power available from the equivalent of lossless half-wave horizontal dipole antennas 23 feet above ground was measured on 2.3, 5.0, and 10.0 MHz at Laem Chabang, Thailand (13.05N°, 100.90°E) from August 1967 through February 1968. Data were obtained using dipoles oriented magnetically north-south (N-S) and east-west (E-W) at the same site where data were being taken with a standard ARN-2 21.75-foot vertical monopole. The noise power available from the dipoles is significantly less than that available from the monopole in the lower part of the HF band, but this difference tends to decrease as frequency increases, becoming negligible at 10.0 MHz at night. The noise picked up by the horizontal dipoles is relatively independent of their orientation, although the E-W dipoles do pick up slightly more noise during winter. The diurnal variation of atmospheric noise observed on the dipoles tends to be greater than that observed on the monopole, and the difference is least on the highest measurement frequency. The noise data from the horizontal dipoles are compared with the CCIR Report 322 predictions for a vertical monopole at the same site, and a correction function is derived to facilitate using those noise maps to make predictions for horizontal dipoles. The effect of local electrical storms on the average noise power observed with the horizontal antennas was studied. It appears that local electrical storms can cause a significant increase in observed average noise power at 2.3 MHz, (that is, more than 20 dB above the monthly median for that hour), but they seem to have relatively little effect at 5.0 and 10.0 MHz (less than 10 dB increase over the monthly median). The observed increases in average noise power during local storms may be smaller than the actual increases in noise-power flux density at the site because of the limitations of our instrumentation. — George H. Hagn, Rangsit Chindahporn, John M. Yarborough.”

Old Noise Data Surfaces

Hagn, et al., conducted experimental measurements for the Stanford Research Institute, US Army Electronics Command, Ft. Monmouth, NJ. Data were taken in Thailand, see the Sidebar for the details. They averaged the measured power over 4 hour time blocks over 8 months, monitoring 2.3, 5 and 10 MHz channels. Table 1 shows a summary of the data based on Figure 16 of the Hagn Report. Comparing dipoles at 23 ft height with a ground mounted vertical,

(1) – A horizontal dipole has up to 20-30 dB (3-5 S units) atmospheric noise advantage over the vertical antenna at the lowest frequency (2.3 MHz), diminishing to only a few decibels at 10 MHz.

(2) – The noise follows the expected 24 thunderstorm cycle (worst at night).

(3) – Measured vertical polarization noise is generally worse than predicated by CCIR 322 / ITU-R-372-9 data.

The overwhelming conclusion is that, for the antenna configurations studied, lower frequencies indeed have lower horizontally polarized atmospheric noise. Happy low frequency DXing!

Robert H Sternowski has held an Amateur Radio license since 1962. After earning his BSEE from the University of Dayton, he worked for Collins Radio and later Rockwell Collins, retiring as an engineering director in 2003. He founded Softronics Ltd in Marion IA, and continues to work in communications system and equipment design. Bob also enjoys his four grandchildren and playing saxophone in a Glenn Miller style big band.

Notes

¹Recommendation ITU-R P.372-9, Radio noise, (Question ITU-R 214/3), 2007.

²G. Hagn, R.Chindahporn and J. Yarborough, "HF Atmospheric Radio Noise on Horizontal Dipole Antennas in Thailand", Special Technical Report 47, Stanford Research Institute, Jun., 1968. DTIC accession number AD681879; www.dtic.mil/dtic/tr/fulltext/u2/681879.pdf.

Book Review

Communication Receivers Principles and Design, by Ulrich L. Rohde, Jerry C. Whittaker and Hans Zahnd

MacGraw Hill 2017, 4th Edition

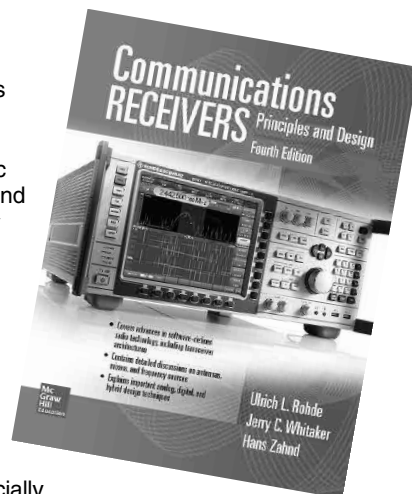
This 4th and brand new edition state-of-the-art book on communications receivers is a comprehensive, one-stop shopping about receivers. Chapter 1 takes the reader into the world of radio receivers by giving a basic introduction into the key signal processing and early history of receivers. This is followed by Chapter 2, which discusses the typical and recommended characteristic of the radio and includes discussion of both signaling (modulation) and the radio channel. The authors address receiver planning for good performance in Chapter 3, and to receiver implementation in Chapters 4. Chapter 5 covers software defined radio (SDR) technologies, implementation and principals. The treatment of SDR, especially Chapter 6 (*transceiver* SDR considerations), benefits from the addition of new co-author Hans Zahnd, HB9CBU, a pioneer developer of SDR-related transceiver designs.

By the time we get to antenna related topics, passive and active antennas of Chapter 7, the content seems firmly organized around systems of a few percent bandwidth, although much wider bandwidth implementations of up to 500 MHz, depending on the RF front end and selected IF bandwidth, are also considered. Chapters 8 – 11 cover real circuitry and measured performance. That is where the authors hold true to the book title.

The evolution from the first edition, which contained all-analog designs, to now all-digital or hybrid (analog/digital) systems, definitely points to a long life for the book. The steps through the four editions chronicle the advance of technology. There is a nice personal touch connecting Ulrich Rohde, DJ2LR, and DJ5LR, his father's call sign, (and now his daughter's call sign) ... "Countless new ideas from a hobby that stayed in the family."

This book is intended as a textbook and includes a huge collection of literature references, with many fundamentals, some of which may get updated every 5 to 10 years.

[Reviewed by Kai Siwiak, KE4PT, QEX Editor.]



Technical Note

A Calculator Solution for Antenna Pattern Peaks and Nulls

You can hand-sketch a very good approximation for the vertical pattern of a horizontally polarized antenna elevated above ground without using any electromagnetic modeling software such as numerical electromagnetic code (NEC). A hand calculator, such as a scientific calculator app on your smart phone, is all you need to find basic pattern features like peak and null angles.

Figure 1 shows the two signal paths transmitted to, or received from, an elevation angle α , for a dipole H_λ wavelengths above ground. The direct and a ground-reflected path lengths differ, and the ground reflected

path undergoes a phase change upon ground reflection. For shallow angles that ground reflection coefficient is -1. So we immediately know that the “zero order null” in the elevation pattern is at $\alpha = 0^\circ$!

The Pattern Nulls

The number of peaks p in a *forward quadrant* of the antenna pattern is,

$$p = 2H_\lambda \quad (1)$$

and p need not be an integer. As H_λ increases, peaks are added gradually from the vertical direction, while the lower angle peaks get compressed. Also, the straight up (90° elevation) peak maximum occurs for antennas that are at even multiples of a half

wavelength minus a quarter wavelength, such as 0.25λ , 0.75λ , 1.25λ , 1.75λ , and so on, as confirmed in the Left and Right plots of Figure 2. When p is a multiple of a wavelength there is a null straight up (Figure 2 Center).

The number of nulls above the zero angle null is the integer part of p . Using simple geometry and image theory, from Figure 1 we see that the ground-reflected path is $2H_\lambda \sin(\alpha)$ longer than the direct path to the distant horizon. The ground reflected path is multiplied by the -1 ground reflection coefficient. The signals along the two paths cancel whenever the added path length, or phase delay, is a multiple m of a wavelength. That is, $2H_\lambda \sin(\alpha) = m\lambda$. Now solve for

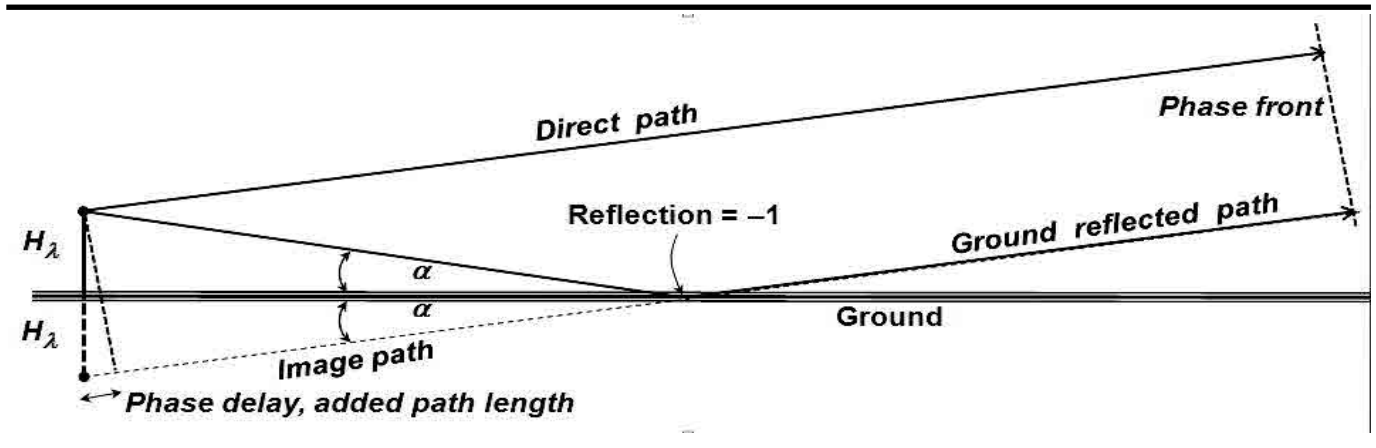


Figure 1 — Geometry for the horizontal antenna above ground.

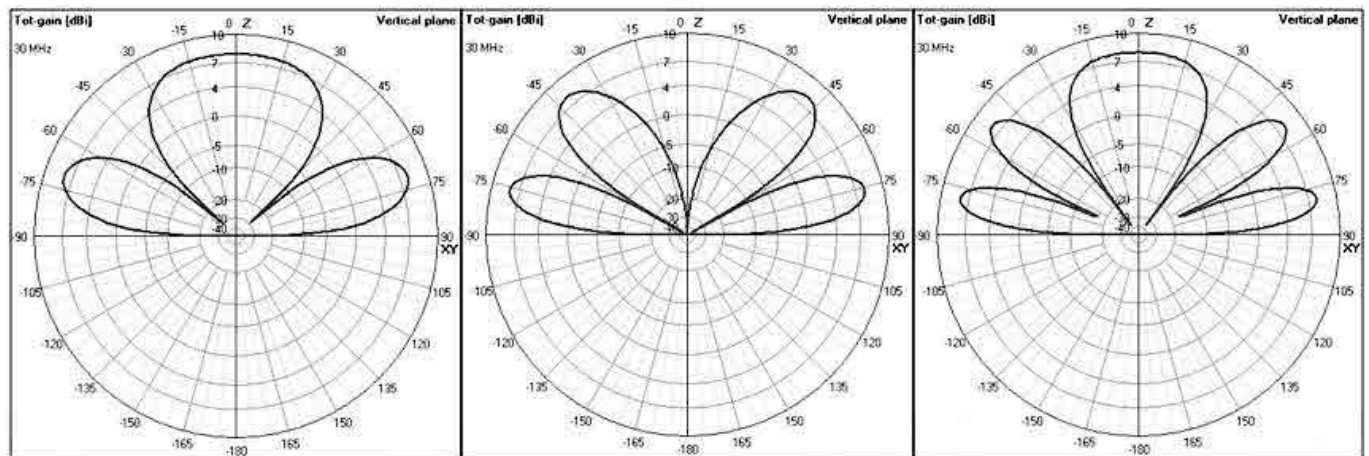


Figure 2 — For a horizontally polarized dipole H_λ wavelengths above ground, use Eq (1), (2) and (3) to discover the number of peaks p , in the forward quadrant, and the null and peak elevation angles α above the horizon. Use NEC with perfect ground to compare. [LEFT] $H_\lambda=0.75$, so $p=1.5$ lobes; my calculator shows peaks at $\alpha=19.5^\circ$ and 90° , and nulls at $\alpha=0^\circ$ and 41.8° . [CENTER] $H_\lambda=1.0$, so $p=2.0$ lobes, with peaks at $\alpha=14.5^\circ$ and 48.6° , and nulls at $\alpha=0^\circ$, 30° and 90° . [RIGHT] $H_\lambda=1.25$, so $p=2.5$ lobes, with peaks at $\alpha=11.5^\circ$, 36.9° and 90° , and nulls at $\alpha=0^\circ$, 23.6° and 53.1° above the horizon.

the angle α of the m^{th} null,

$$\alpha_{m_NULL} = \arcsin(m/2H_\lambda) \quad (2)$$

Use a simple scientific calculator with the inverse sine function to find the angles of the m nulls.

The Pattern Peaks

The signals via the two paths combine constructively to double the field strength (+6 dB above the free space value) for a perfect ground — or about 4 to 5 dB for medium ground — whenever the path difference, or phase delay, is an odd multiple m of a half wavelength. That is, $2H_\lambda \sin(\alpha) = (2m-1)/\lambda$. Solve for the angle α ,

$$\alpha_{m_PEAK} = \arcsin((2m-1)/4H_\lambda) \quad (3)$$

which is easily computed on a scientific calculator using the inverse sine function!

Verify with NEC

You can verify scenarios of the dipole at 0.75, 1.0, and 1.25 λ above the ground (Figure 2). Use Eq (1) to calculate the number of nulls p in the forward quadrant, and then Eq (2) and (3) to find the elevation angles above the horizon of the nulls and peaks. Nulls are very deep with a perfect ground. With a medium ground, the higher elevation nulls are not as deep and peaks are slightly less pronounced, but angles still match. Apply these peak and null angles to any horizontally polarized antenna above ground. — *Best regards, Kai Siwiak, KE4PT.*

Send your short *QEX* Tech Note to the Editor, via e-mail to qex@arrrl.org. We reserve the right to edit your letter for clarity, and to fit in the available page space. “*QEX* Tech Note” may also appear in other ARRL media. The publishers of *QEX* assume no responsibilities for statements made by correspondents.

**We Design And Manufacture
To Meet Your Requirements**

**Prototype or Production Quantities*

800-522-2253

**This Number May Not
Save Your Life...**

**But it could make it a lot easier!
Especially when it comes to
ordering non-standard connectors.**

RF/MICROWAVE CONNECTORS, CABLES AND ASSEMBLIES

- Specials our specialty. Virtually any SMA, N, TNC, HN, LC, RP, BNC, SMB, or SMC delivered in 2-4 weeks.
- Cross reference library to all major manufacturers.
- Experts in supplying “hard to get” RF connectors.
- Our adapters can satisfy virtually any combination of requirements between series.
- Extensive inventory of passive RF/Microwave components including attenuators, terminations and dividers.
- No minimum order.

NEMAL
 **Cable & Connectors**
for the Electronics Industry

NEMAL ELECTRONICS INTERNATIONAL, INC.
12240 N.E. 14TH AVENUE
NORTH MIAMI, FL 33161
TEL: 305-899-0900 • FAX: 305-895-8178
E-MAIL: INFO@NEMAL.COM
BRASIL: (011) 5535-2368

URL: WWW.NEMAL.COM

From **MILLIWATTS**
To **KILOWATTS**SM
*More Watts per Dollar*SM

In Stock Now!
**Semiconductors
for Manufacturing
and Servicing
Communications
Equipment**

- **RF Modules**
- **Semiconductors**
- **Transmitter Tubes**

Se Habla Español • We Export

Phone: **760-744-0700**

Toll-Free: **800-737-2787**

(Orders only) **800-RF PARTS**

Website: **www.rfparts.com**

Fax: **760-744-1943**

888-744-1943

Email: **rfp@rfparts.com**



RF **RF PARTS**
COMPANY
From Milliwatts to KilowattsSM

Letters to the Editor

Radio Frequency (RF) Surge Suppressor Ratings for Transmissions into Reactive Loads (Jul/Aug 2016)

Note 8, the source for Gene Hinkle's Equation (2), was inadvertently omitted. It should be, ⁸*The ARRL Antenna Book*, 23rd Edition, p. 23-13, (Eq. 18). — Ed.

Staggered Resonator Filters using LC Resonators (Sep/Oct 2016)

Dear Editor,

The rule to be followed in designating and placing the components, as in Figure 1 of the Gary Appel, WAØTFB, article is to place the *C* or *L* with even numbers in the series branches and odd numbers in the shunt branches. In the four shunt branches of Figure 1, the labels left to right should be *C1* and *L1*, then *C3* and *L3*, *C5* and *L5*, ending with *C7* and *L7*. If the first component starts as a series component, the labeling is different and the rule is modified to account for this. All components take the number of the branch it is in. There are three series branches in Figure 1, and the series components are labeled as *L2*, *C4* and *L6*. Note that the four shunt resonators have the same numbers for the *C* and *L* components. Also in Figure 1 there are no source and load impedances specified.

Mr. Appel ignores the filter design work of Jim Tonne, W4ENE, that is published on a disk that is placed the *ARRL Handbook*. Tonne's references should have been used because the author's listed references are not conveniently available to the *QEX* readers. — 73, Ed Wetherhold, W3NQJ, *ARRL Technical Advisor*.

[The author replies],

Thank you for your comments on the correct designation of components in the filter shown in Figure 1. I will keep that in mind for future reference. You also noted that I did not supply the source and load impedances for the coupled resonator filter in Figure 1. This was certainly an oversight. This filter was designed to operate between a source and load impedance of 1 kΩ.

As far as the references I included, these are the resources that I used in developing my design. As such, they were included as references to the article. While many other excellent references are available, these references are also valuable. In particular the *Reference Data for Radio Engineers*, Fifth Edition, discusses the implementation

of the mixed coupling shown in Figure 1, which is not commonly discussed. The two referenced books should be easily located using the Internet, if desired.

Thank you for your comments, I hope that some of our community finds the information presented in this article to be interesting, and perhaps even useful. — Gary Appel, WAØTFB.

A More Efficient Low-pass Filter (Nov/Dec 2016)

Dear Editor,

The Gary Cobb, G3TMG, filters are impressive for their performance, but they use mostly non-standard value components. I designed a 2nd harmonic trap circuit comprising a standard value 0.68 μH inductor and a 188 pF capacitor (four 47 pF capacitors in parallel), with 228 pF input shunt and 232 pF output shunt capacitors, which may be appended to any other 50 Ω filter. Values are for 40 m but you can scale them to other frequencies by multiplying the values by the ratio of 7.1 divided by the new frequency. Then tweak the values in filter design software to place the notch and best return loss where you want them. If you put this circuit on the output end of your filter and use variable capacitors for the input and output shunt capacitors, it can double as a tuner. It will attenuate the 2nd harmonic by more than 40 dB from what it was before and all higher frequencies by at least 12 dB, enabling an otherwise marginal filter to greatly exceed FCC requirements. Insertion loss is 0.03 dB at 7 MHz increasing to 0.04 dB at 7.3 MHz. — 73, Joe Stern, K14QG, ki4qg@twc.com.

[The author replies]

Joe has a most logical approach to the harmonic suppression problem, but I think that he has missed the point of the article, which is about efficient designs. Efficiency, in this case, is about the minimum number of components needed in respect of the realizable performance that can be achieved. The values in the published Table 3 of the *QEX* article are, of course, ideal and represent target values. Depending on how these desired values are contrived, the realized response will be achieved with a certain number of actual components which most often exceeds the ideal minimum. This is the preferred value issue and I make no attempt to deal with this because it is certainly not trivial. I think that the ideal value Table gives prospective users the widest possible range of choices, which may include parasitics, on how to physically

realize a ZWAZ filter network.

Interestingly, I note that even Joe uses four 47 pF *zero tolerance* capacitors to make up his 188 pF trap capacitor ideal value. Also, his input and output shunt capacitors are 228pF and 232pF respectively, which are also non-standard values. Yes, the 0.68 μH inductor mentioned is a standard value but what of its tolerance? My article does what it says, which is to compare the ZWAZ quasi-elliptic design against the classical Chebyshev low-pass filter approach. If any polynomial approximated network is designed from first principals, non standard values would be obtained. On the way through, the article discusses Jim Tonnes CWAZ designs (limited to $N=5$), which are also clearly quasi-elliptic. The initial design, using his OptLowpass program, also starts by generating the ideal values. He then provides a facility of selecting the nearest preferred value for each element and, by analysis, shows the response degradation as compared to the ideal approximated one. As mentioned in my article, this can be carried out using any of the freely available circuit simulators.

The work reported in my article was carried out using the concept of a single Zolotarev functional approximation yielding a straight-forward circuit synthesis. Of course, cascading filter functions can achieve almost any desired response but, is it efficient?

To utilize Joe's approach and notionally the same number of components as the $N=7$ ZWAZ demonstrated in my article, we would require a 5th order Chebyshev low-pass filter followed by Joe's 3 component independently designed trap — the first shunt *C* being absorbed into the Chebyshev network. The result is found to be very comparable to the CWAZ response of Figure 4 of my article (divide the frequency scale by a factor of 10) except that the pass-band return-loss is not so well behaved. Therefore, the comparison of Joe's proposed approach and the new ZWAZ design is pretty much as indicated in Figure 9(B), showing a significant difference as indicated in the concluding remarks of my *QEX* article. — Regards, Gary Cobb, G3TMG.

A Study of Long Path Echoes (Jan/Feb 2017)

Dear Editor,

Thank you for the several fine articles on propagation. The attached image (Figure A) with its original caption is nearly 90 years old, and considering the primitive state

of that technology I find it amazing how similar it is to the Flavio Egano, IK3XTV, Figure 1. Clearly our desire to understand the ionosphere continues. — 73, Ron Skelton, W6WO.

[Thanks Ron, The image you found appeared in “A Treatise on Short Waves,” by Dr. H. Bley, in *Short Wave Craft*, June/July, Vol. 1, No. 1, 1930. It was indeed a very interesting observation from an early time period — Ed.]

[The author replies]

It is amazing to me to discover that almost 90 years ago some people were already able to make these measurements. — *Thanks and 73, Flavio Egano, IK3XTV.*

A Different Approach to Yagi-Uda Antenna Design (Jan/Feb 2017)

Dear Editor,

I read with interest the article by Robert J. Zavrel, W7SX. Revolutionary advances in antenna design are truly rare. The Yagi-Uda array is approaching its 100-th birthday and the LPDA is now about 60 years old. Zavrel was modest in calling his idea a different Yagi-Uda. While it is, I suppose, a variation on the classic, Zavrel’s design will forever in my mind be a *W7SX Array*. It solves many problems of a rotatable directive-array covering 5 bands with a 40 m dipole bonus.

The best engineering designs involve tradeoffs. By abandoning a desire for a 50 Ω feed point match, recognizing the advantages of longer elements, and accepting only reflector parasitics, Zavrel achieved a directive 5-band antenna on a very short boom with fewer traps. Wow! The extreme SWR and open-wire feed line for a rotatable antenna do create challenges, but resourceful amateurs will most certainly overcome those challenges. Zavrel’s ideas are general enough that the future will see many variations on the W7SX design.

I love symmetry, but the complexity of the W7SX traps can be reduced by abandoning symmetry. Because the entire trap assemblies are only two-terminal networks, symmetry is not required. I’m certain the two 19 pF capacitors in Figure 1 may be replaced with

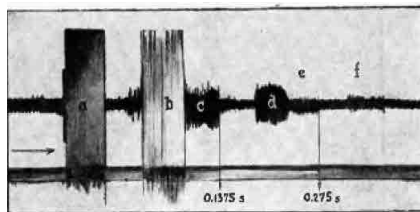


Fig. 3. A most astonishing oscillogram or graphic curve showing the actual record of a radio signal which has encircled the earth not only once, but twice! In the illustration, a and b indicate the signals arriving over the shortest path; c and d indicate the signals which went around the earth once; while e and f are the records of the radio signals which went around the earth twice!

Figure A — [Source: *Short Wave Craft*, Vol. 1, No. 1, 1930.]

one 9.5 pF capacitor, the two 5 μH inductors in Figure 2 may be replaced with one 10 μH inductor, and the two 15 pF capacitors may be replaced with one 7.5 pF capacitor.

Thanks to Robert for his insight and to *QEX* for continuing to publish innovation. — *Randy Rhea, N4HI.*

[The author replies]

Randy, thank you very much for your very kind words, I am glad you enjoyed this paper. Regarding symmetry, yes you are correct that the traps could be simpler (asymmetric). However, I chose symmetry mainly for the bands where the LC tank breaks the parasitic element into two co-linear elements. On these bands asymmetry would result in different lengths for the two sides of the element, since the series inductor and capacitor have physical lengths. This would not be much of a problem on the other bands. Also they have weight, which would mean one side of the element would be slightly heavier than the other. Otherwise, there is no reason for, as you suggest, not using an asymmetric arrangement of the lumped components comprising the traps. Thanks again for you the note. — 73, Bob Zavrel, W7SX.

Send your *QEX* Letters to the Editor to, ARRL, 225 Main St., Newington, CT 06111, or by fax at 860-594-0259, or via e-mail to qex@arrl.org. We reserve the right to edit your letter for clarity, and to fit in the available page space. “Letters to the Editor” may also appear in other ARRL media. The publishers of *QEX* assume no responsibilities for statements made by correspondents.

From **MILLIWATTS**
To **KILOWATTS**
More Watts per Dollar

Transmitting & Audio Tubes

**COMMUNICATIONS
BROADCAST
INDUSTRY
AMATEUR**

Immediate Shipment from Stock

3CPX800A7	4CX1000A	810
3CPX1500A7	4CX1500B	811A
3CX400A7	4CX3500A	812A
3CX800A7	4CX5000A	833A
3CX1200A7	4CX7500A	833C
3CX1200D7	4CX10000A	845
3CX1200Z7	4CX15000A	6146B
3CX1500A7	4CX20000B	3-500ZG
3CX3000A7	4CX20000C	3-1000Z
3CX6000A7	4CX20000D	4-400A
3CX10000A7	4X150A	4-1000A
3CX15000A7	572B	4PR400A
3CX20000A7	805	4PR1000A
4CX250B	807	...and more!

Se Habla Español • We Export

Phone: 760-744-0700

Toll-Free: 800-737-2787
(Orders only) **RF PARTS**

Website: www.rfparts.com

Fax: 760-744-1943
888-744-1943

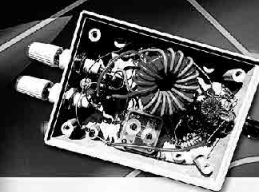
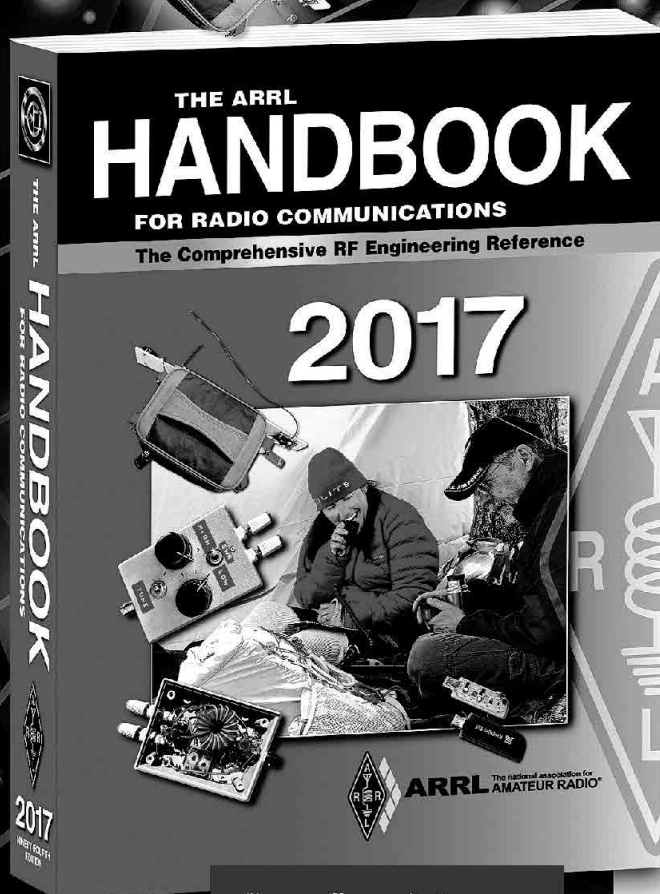
Email: rfp@rfparts.com

Advancing Radio Science and Technology

THE ARRL HANDBOOK

FOR RADIO COMMUNICATIONS

2017



The ARRL Handbook is the standard for applied theory and practical information concerning the fundamentals of radio electronics, circuit design and equipment, radio signal transmission and propagation, antennas, construction practices, and much more. Each chapter is filled with the most up-to-date knowledge representative of the wide and ever-expanding range of interests among radio amateurs. There are practical, hands-on projects for all skill levels, from simple accessories and small power supplies, to legal-limit amplifiers and high-gain antennas.

This 94th edition of **The ARRL Handbook** is a cornerstone of radio experimentation, discovery, and achievement. First introduced in 1926 as *The Radio Amateur's Handbook*, today's **Handbook** is a comprehensive technical reference used by radio amateurs, experimenters, students, and practicing engineers.

New projects and information include...

- Revised Approach to Measuring Crystal Parameters
- High-Performance IF and Dual-band Preamp Project
- Decoding Fox-1 Satellite Telemetry
- RTL-SDR Receiver Project
- Updated Predictions for Solar Cycle 24 and Beyond
- Updated Details on the Placement of Filter Stubs
- 30, 17, and 12 Meter Antenna Project

CD-ROM Inside

Includes fully searchable text and illustrations, expanded supplemental content, software, PC board templates, and other support files.

Hardcover Handbook

Book with CD-ROM

ARRL Item No. 0635

Bonus! Only \$49.95*

Retail \$59.95—ends 4/30/2017

Softcover Handbook

Book with CD-ROM

ARRL Item No. 0628

Only \$49.95*

"I can offer no better recommendation of the Handbook than to say that it teaches us the 'what' and the 'how-to' about radio technology."

Tom Gallagher, NY2RF
ARRL Chief Executive Officer

Companion Books Available:

The ARRL Operating Manual for Radio Amateurs

The ARRL Antenna Book for Radio Communications

*plus shipping and handling



ARRL The national association for
AMATEUR RADIO®

www.arrl.org/shop

Toll-Free US 888-277-5289 or
elsewhere +1-860-594-0355

Every Ham Needs This Essential Book!

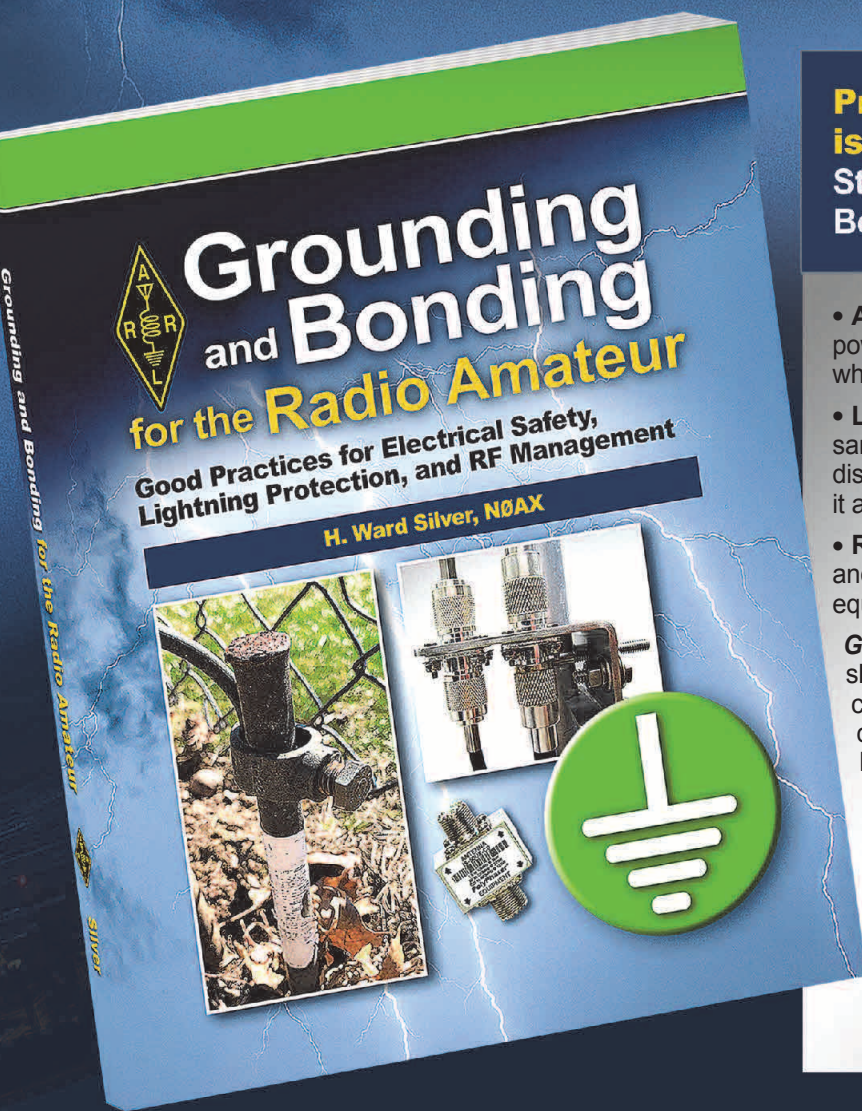


Grounding and Bonding for the Radio Amateur

H. Ward Silver, NØAX



Good Practices for Electrical Safety,
Lightning Protection, and RF Management



Proper Station Grounding is Important!... Build Your Ham Radio Station with Effective Grounding and Bonding Techniques:

- **AC safety:** protects against shock hazards from ac-powered equipment by providing a safe path for current when a fault in wiring or insulation occurs.
- **Lightning protection:** keeps all equipment at the same voltage during transients from lightning and dissipate the lightning's charge in the Earth, routing it away from equipment.
- **RF management:** prevents unwanted RF currents and voltages from disrupting the normal functions of equipment (also known as RF interference or RFI).

Grounding and Bonding for the Radio Amateur shows you how to make sure your station follows current standards for lightning protection and communication systems, not to mention the National Electrical Code. You'll learn effective grounding and bonding techniques for home stations, including condos and apartments, portable and temporary stations, as well as towers and outside antennas.

Grounding and Bonding for the Radio Amateur

ARRL Item No. 0659

ARRL Member Price! Only \$22.95
(retail \$25.95)



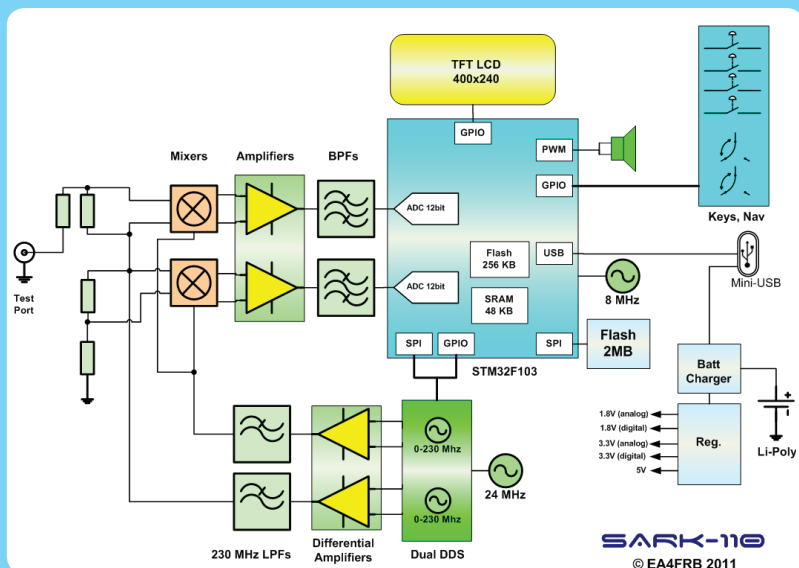
ARRL The national association for
AMATEUR RADIO®

www.arrl.org/shop

Toll-Free US 888-277-5289,
or elsewhere +1-860-594-0355

QEX 5/2017

SARK-110 Versatility: From Tower to Test Bench



The SARK-110 is more than just an antenna analyzer. It's a multi-use precision instrument capable of analyzing antennas or networks, generating or detecting signals, performing TDR measurements on transmission lines, and displaying information in XY or Smith chart formats, between 100 kHz and 230 MHz.

The SARK-110 is small: it weighs less than 4.5 ounces, including the built-in rechargeable battery. You can perform measurements on the go and save them in the built-in storage for later upload to your computer through the built-in USB interface.



For bench applications, the SARK-110 can be controlled from your desktop computer via the USB interface. Display shows on computer.

SteppIR
Antenna Systems

The SARK-110 is upgradeable. As necessary, new firmware releases are made available on SARK110.com, where you can also find other resources such as application notes. If you have a special purpose in mind, you can even program the SARK-110 with your own application using the SDK available on the website.

Order your SARK-110 today - \$389.00
www.steppir.com/steppir-sark-110

